Fermilab Muon g-2 Experiment

Ritwika Chakraborty

University of Kentucky/Paul Scherrer Institute

19th December 2022

g-factor of charged leptons

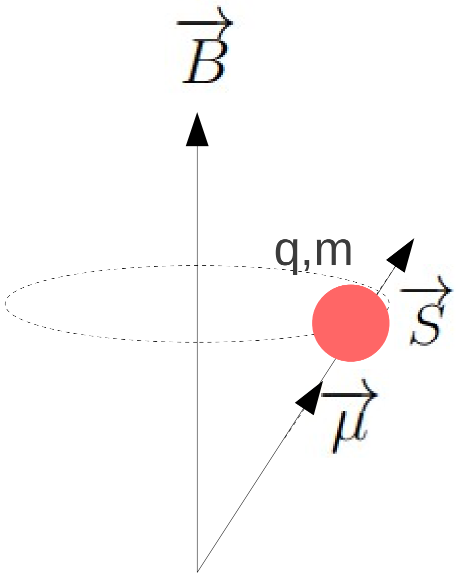

- Leptons have magnetic moment due to spin

$$\overrightarrow{\mu} = g\frac{q}{2m}\overrightarrow{S}$$

- When placed in external magnetic field, undergo Larmor precession

$$\overrightarrow{\omega_s} = \frac{gq}{2m}\overrightarrow{B}$$

- g-factor affects rate of precession, denotes strength of interaction between spin and magnetic field

Numerical value of g

- Experiments with atoms in magnetic field indicated g = 2, example anomalous Zeeman effect
- Ad-hoc assumption
- First robust theoretical prediction given by Dirac
- For a spin ½ point particle in EM potential

$$\gamma^\mu(i\partial_\mu - eA_\mu)\psi(x) - m\psi(x) = 0$$

where it can be shown that

$$g = 2$$

Deviation from g=2

- Experimentally deviation of g-factor of electron from 2 was observed in hyperfine splitting experiments

- Kusch and Foley measured it in 1947 and found

$$g = 2(1 + 0.00119) \pm 0.0001$$

- In 1948, Schwinger explained the interaction to be electron *self-interaction*

- Precisely calculated the deviation to be

$$g = 2(1 + \underline{0.0011614})$$

$$\downarrow$$

$$\boxed{\frac{\alpha}{2\pi}}$$

Schwinger term

Muon g-2 Theory

Quantum Electrodynamics

Feynman diagrams with leptonic and photonic loops

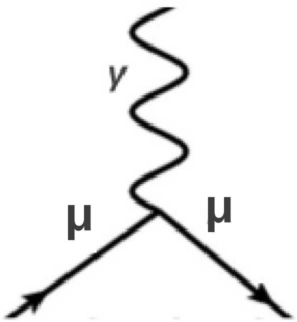

$$a_\mu = \frac{g-2}{2} = 0$$

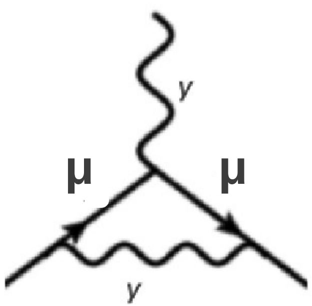

$$a_\mu = \frac{g-2}{2} = \frac{\alpha}{2\pi}$$

Muon g-2 Theory

Quantum Electrodynamics

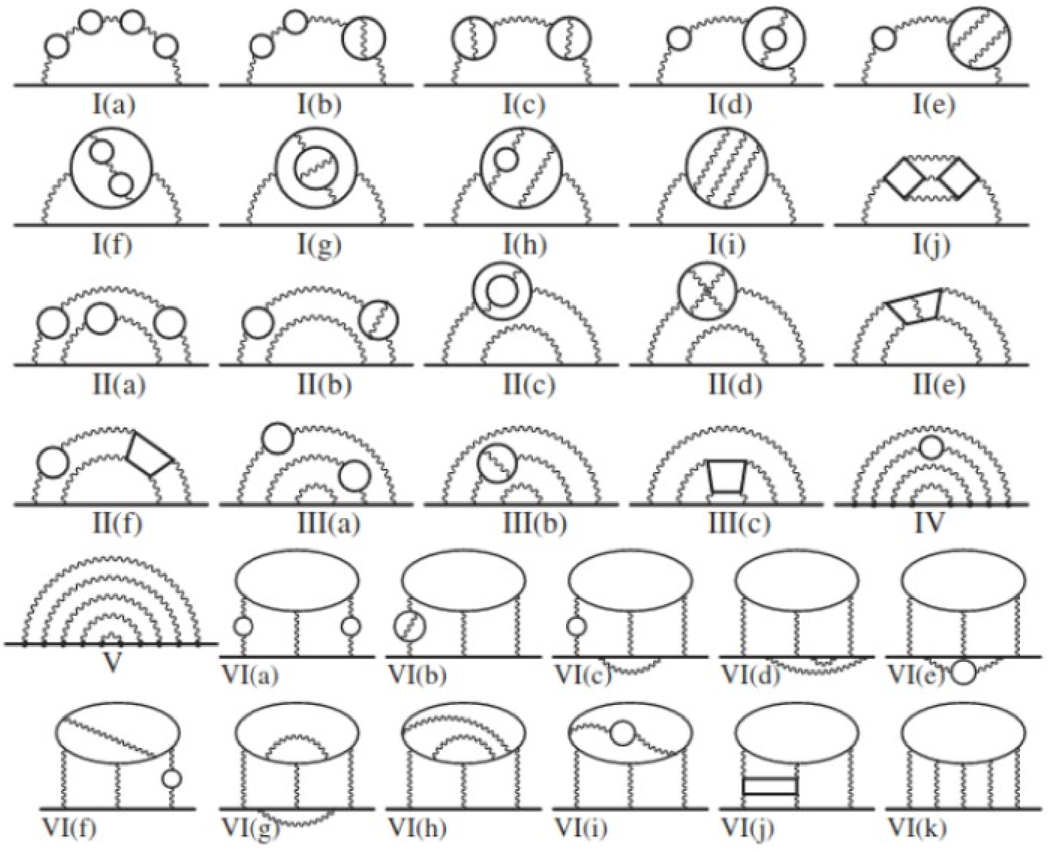

- Currently calculated upto order 5-loops

$$a_\mu^{QED} = 116584718.931(104) \times 10^{-11}$$

Muon g-2 Theory

Electro-weak contributions

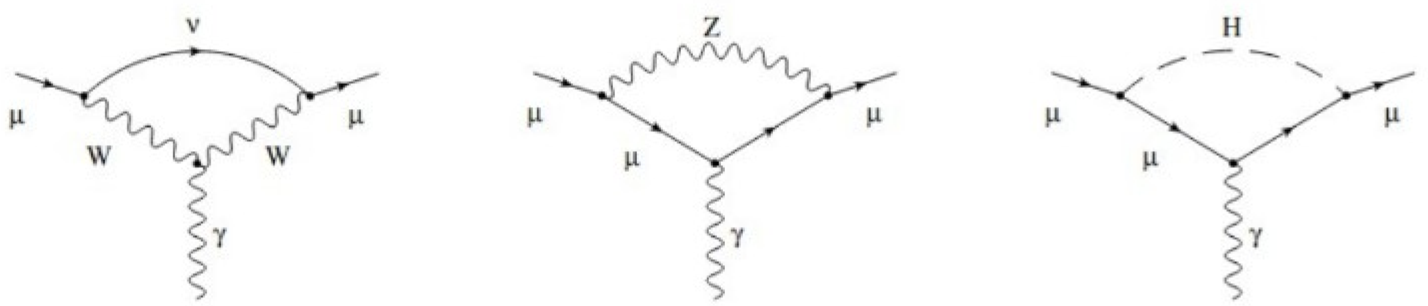

- Currently calculated upto order 2-loop
- Higher order contributions highly suppressed

$$\boxed{a_\mu^{EW} = 153.6(1.0) \times 10^{-11}}$$

Muon g-2 Theory

Hadronic contributions

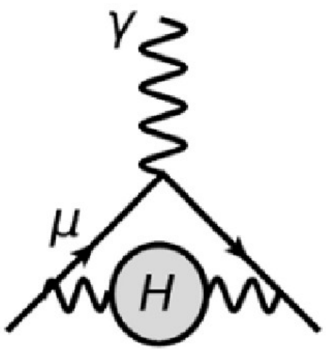

Hadronic vacuum polarization

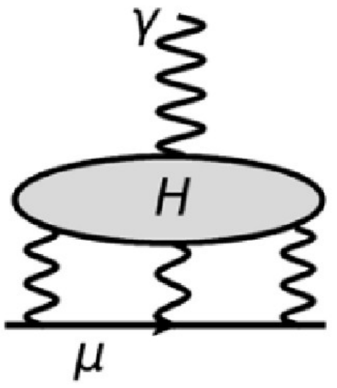

Hadronic light-by-light

- Evaluated using dispersion integrals involving data driven cross sections
- Lattice calculations have recently become promising

$$\boxed{a_\mu^{HVP,LO} = 6931(40) \times 10^{-11}}$$

$$\boxed{a_\mu^{HLbL,LO} = 92(19) \times 10^{-11}}$$

Muon g-2 Theory

Standard Model Contributions

$$a_\mu^{SM} = a_\mu^{QED} + a_\mu^{EW} + a_\mu^{Had}$$

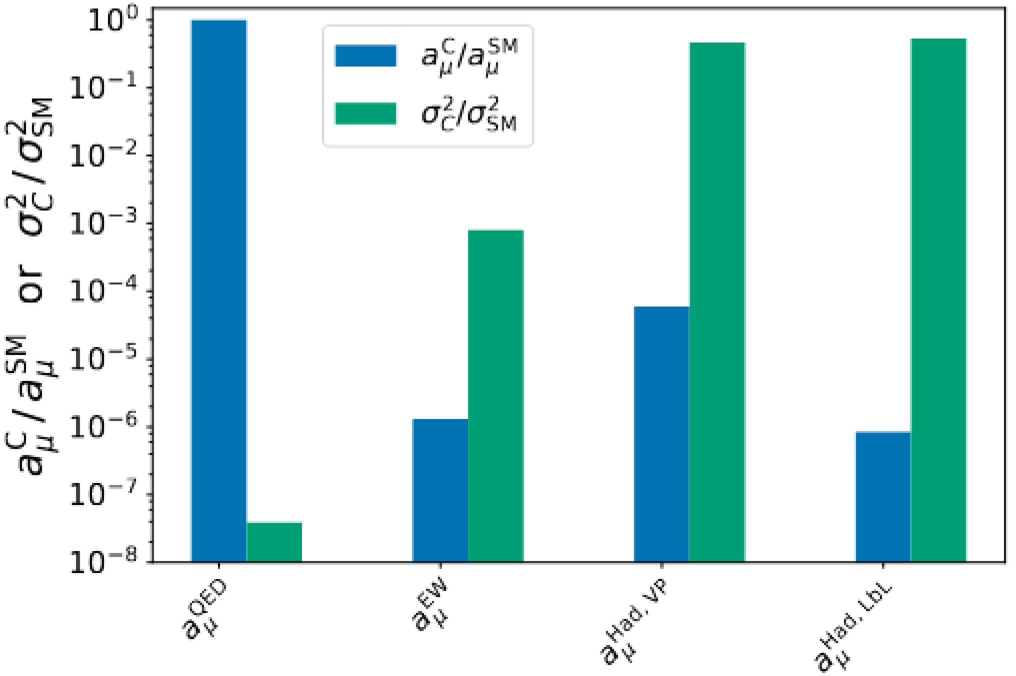

Muon g-2 Theory Initiative 2020

$$a_\mu^{SM} = 116592089(63) \times 10^{-11}$$

Comparison with Muon g-2 Experiment

- Series of experiments in CERN 1960-1979
- More recently most precise experiment at BNL (540 ppb)

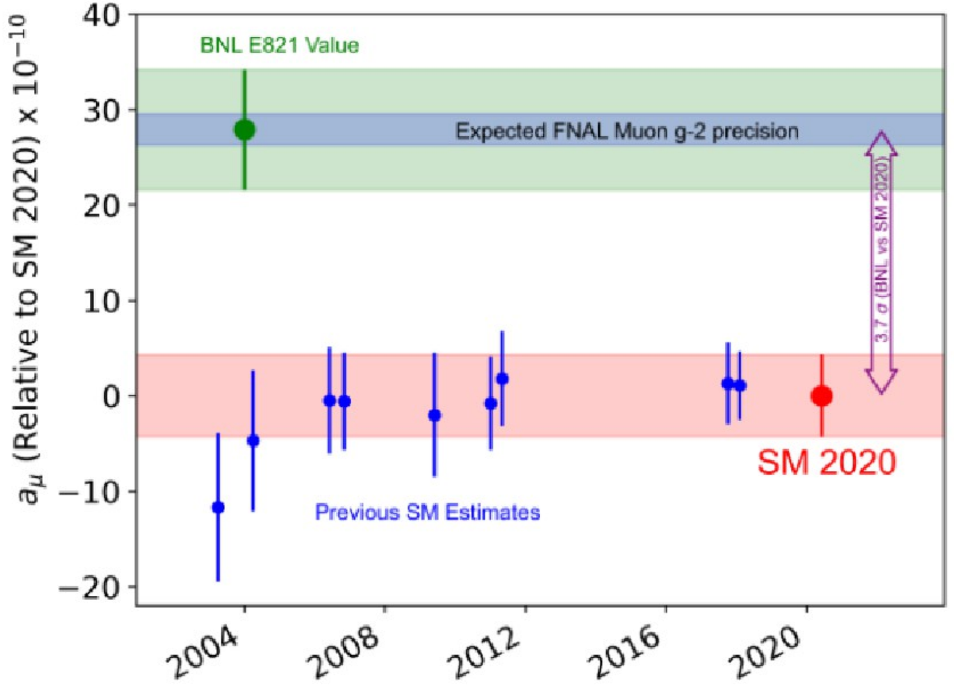

- 3.7 sigma discrepancy with 2020 theory value, BSM physics?
- Need for improving precision on experiment

Fermilab Muon g-2 Experiment

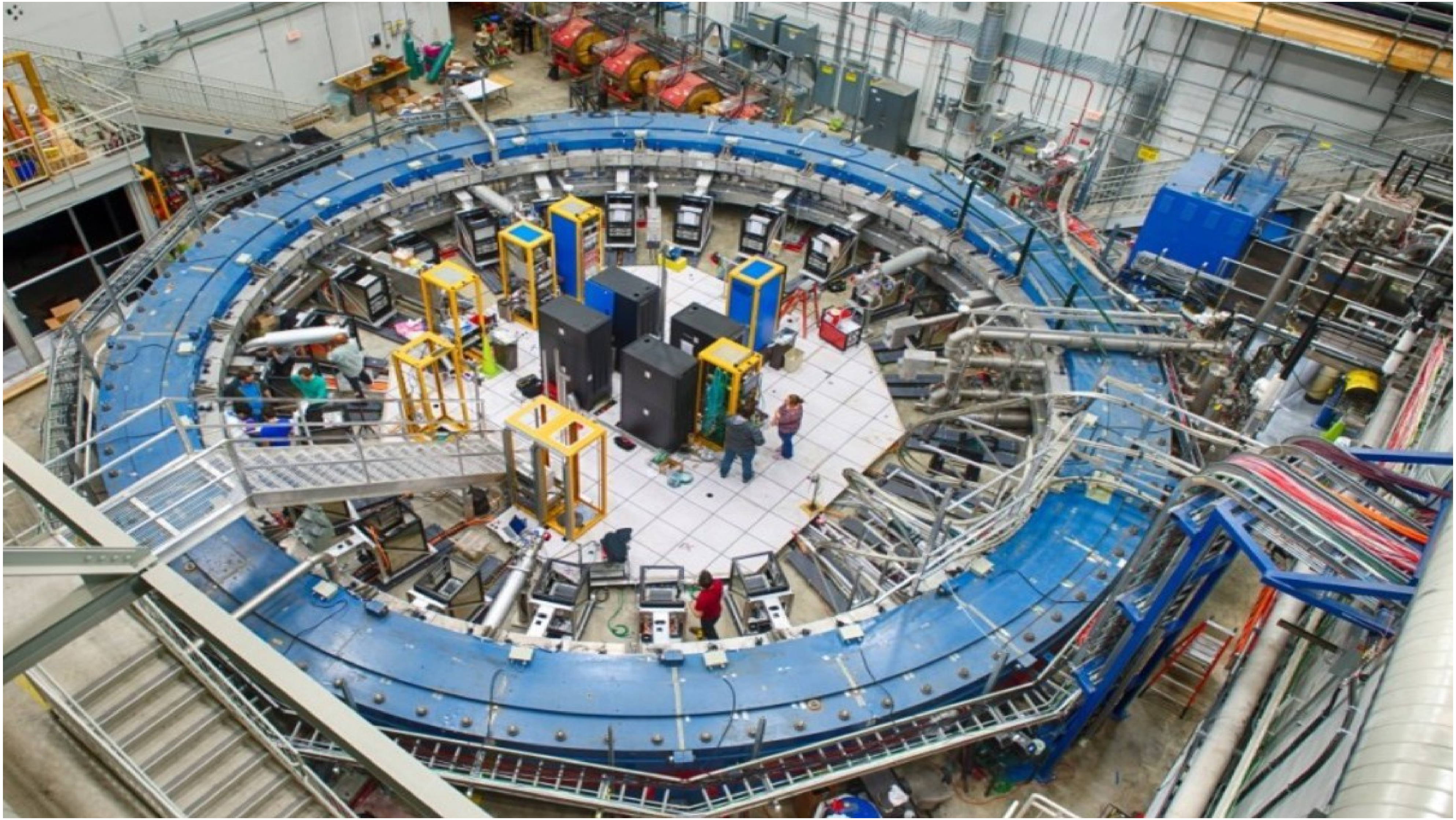

The Magnet

- C-shaped magnet provides 1.45 T dipole field in the ring of radius 7.115 m

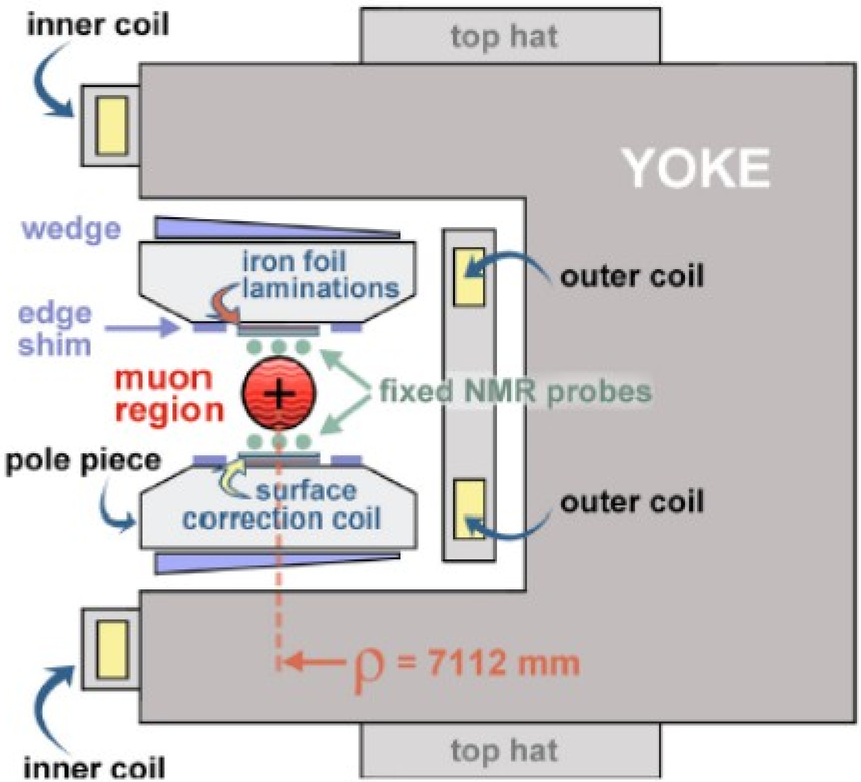

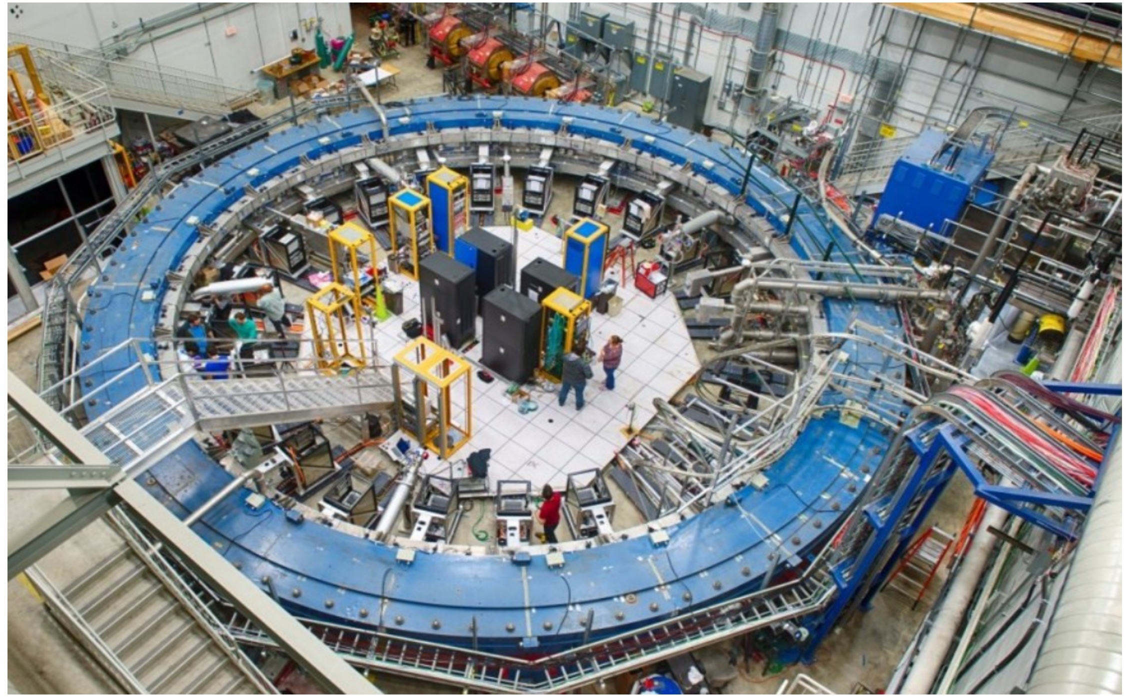

- Iron shims to achieve field uniformity of ±25 ppm

Inflector Magnet

- Muons need to be injected to the storage ring through a field free region

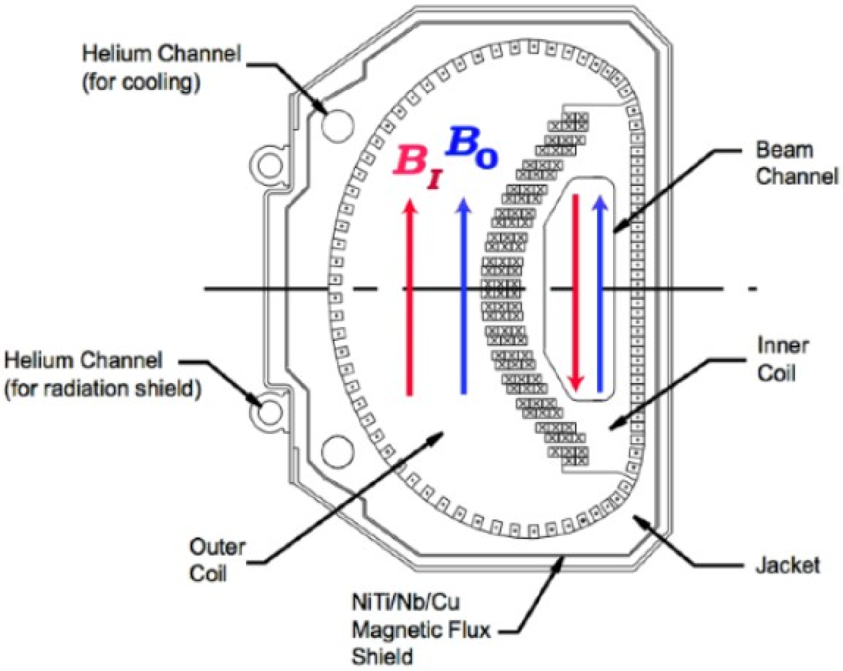

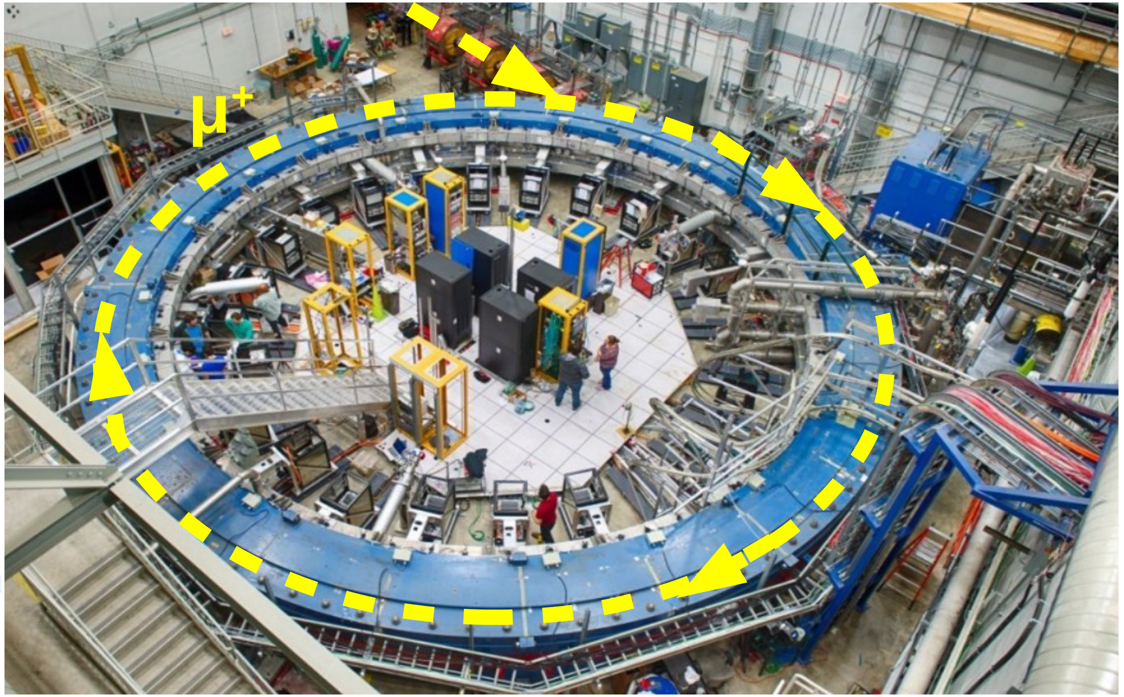

- The inflector magnet cancels out the 1.45 T dipole field at the point of injection

Kicker Magnet

- Muons are kicked onto the storage orbit by magnetic plates called kicker

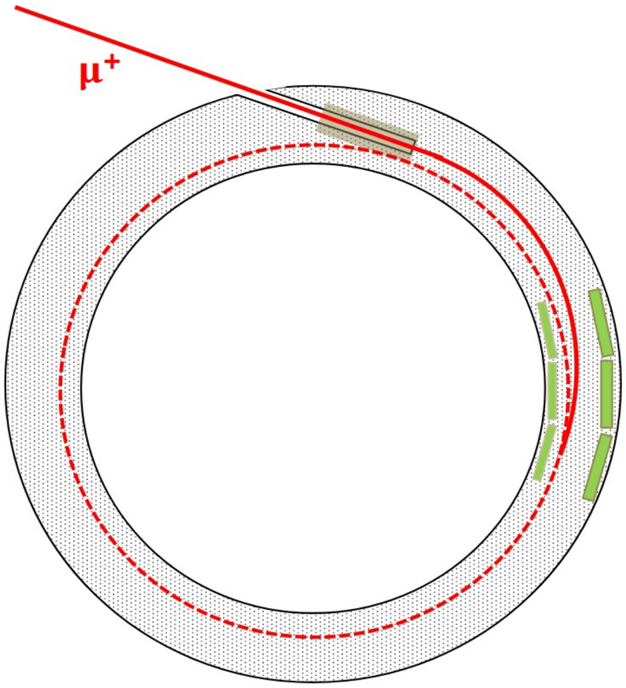

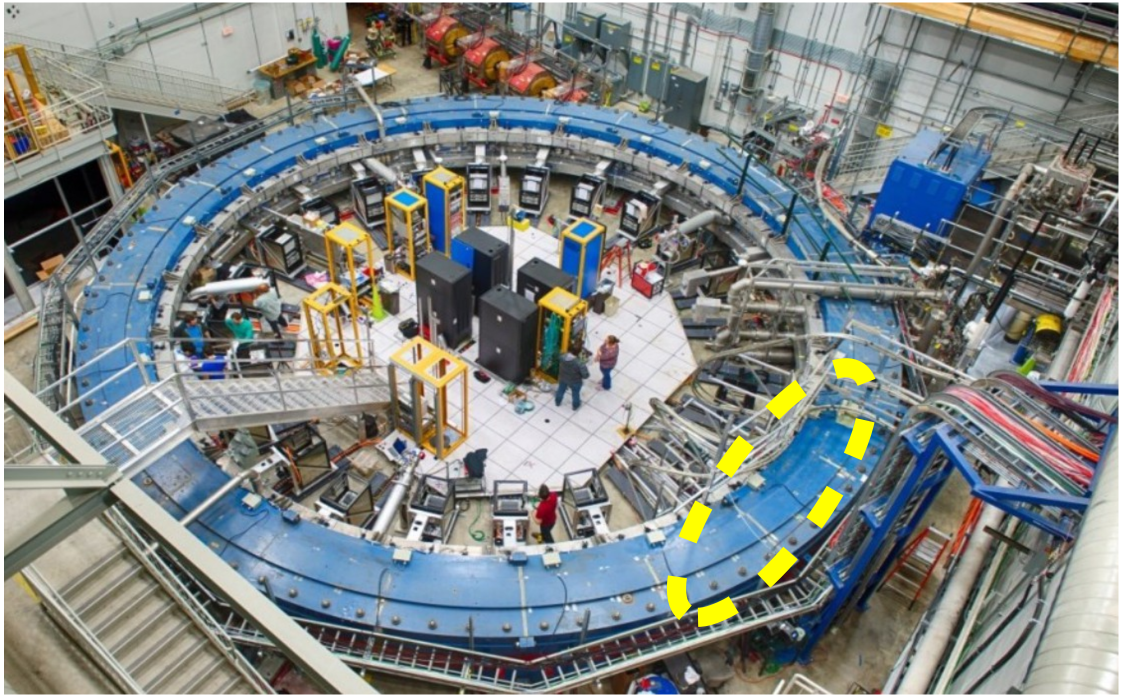

Electro-static Quadrupole (ESQ)

- 4 pairs of high voltage quad-rupole plates
- Provides restoring force in the vertical direction

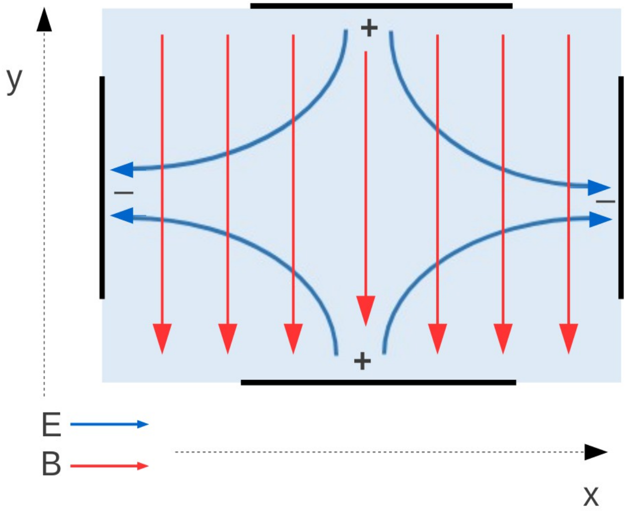

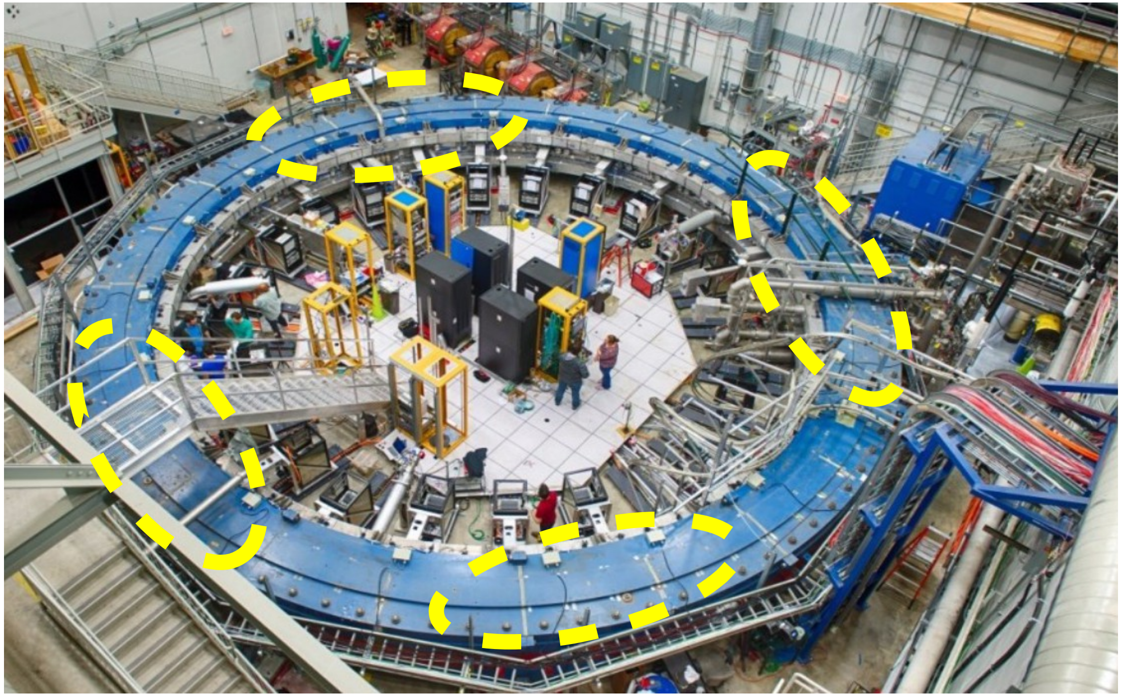

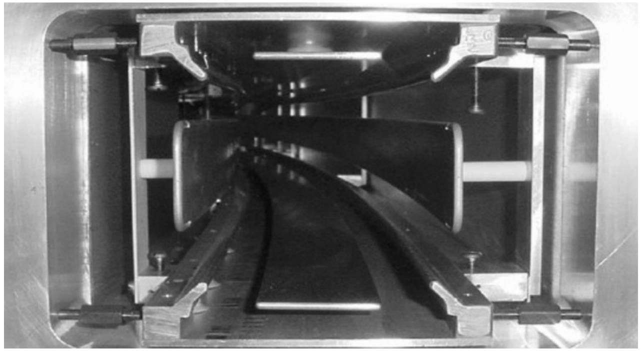

Calorimeter Detectors

- Muons decay into positrons and neutrinos

$$\mu^+ \rightarrow \bar{\nu_\mu} + e^+ + \nu_e$$

- The positrons hit the 24 calos and generate Cherenkov shower

- Detected by SiPMs

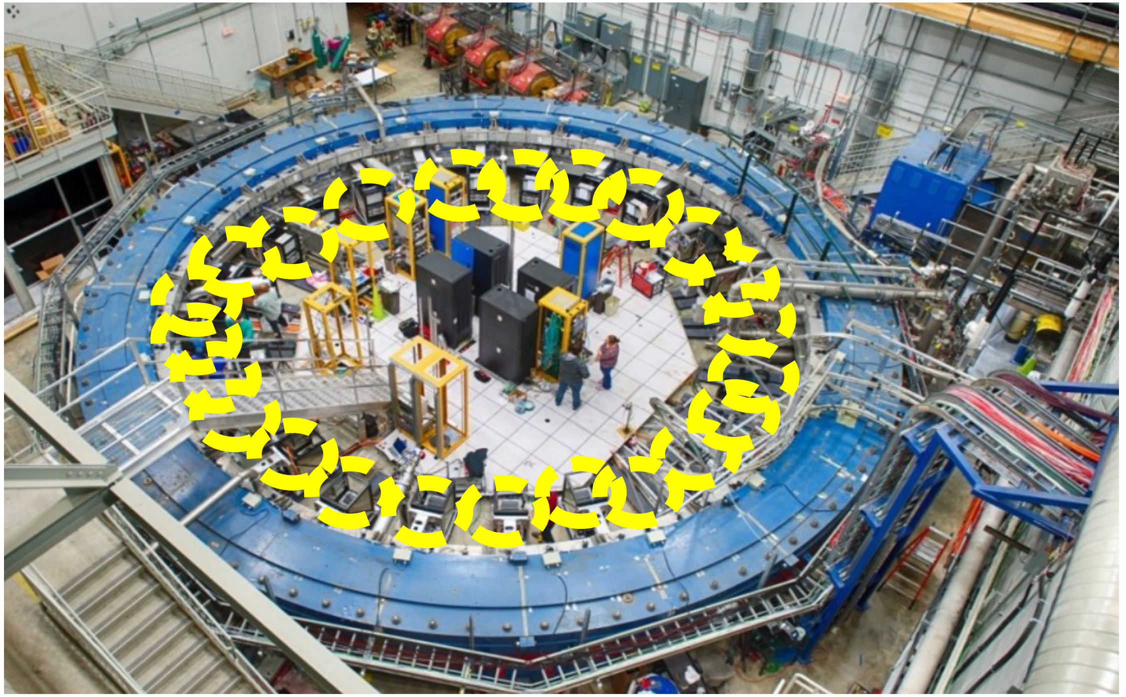

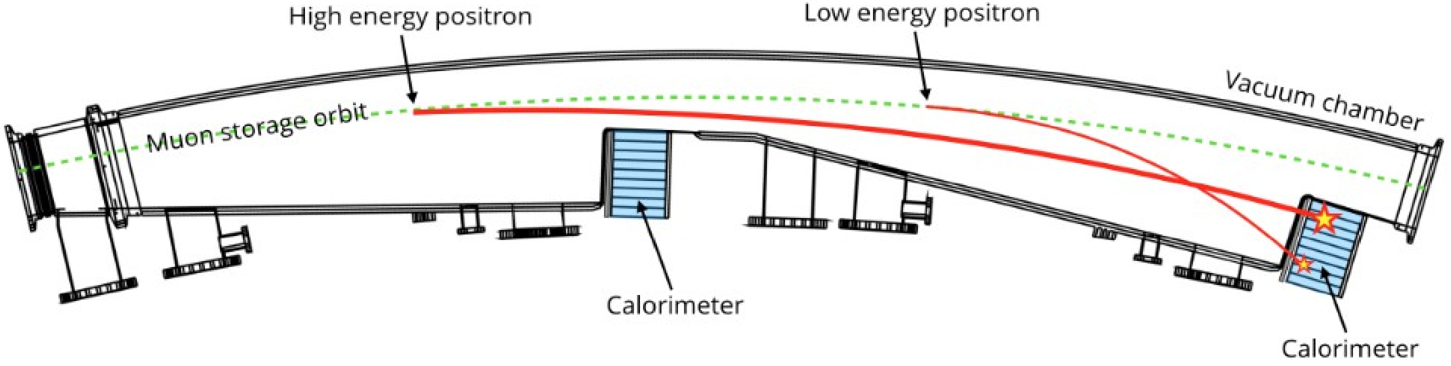

Trackers

- Two straw tracker stations in front of calo 12 and 18
- Each has 8 modules with 128 straw chambers

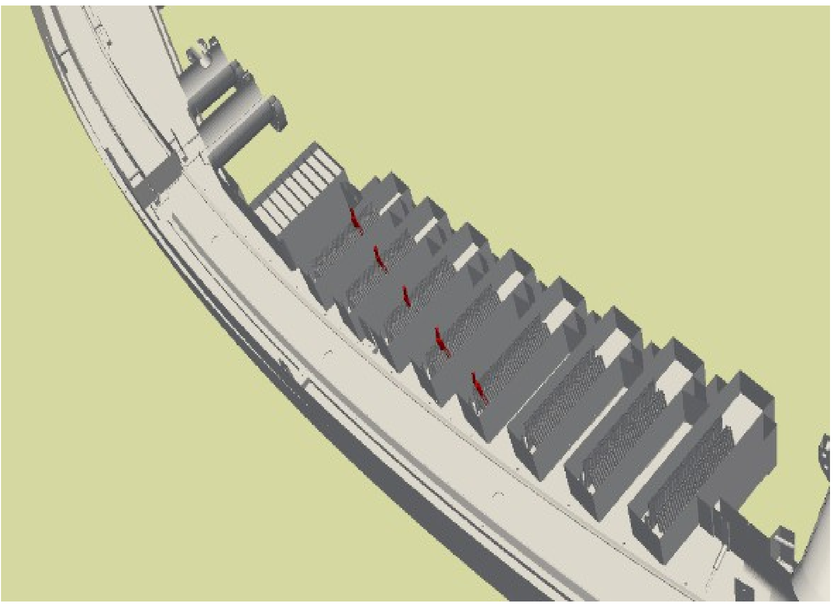

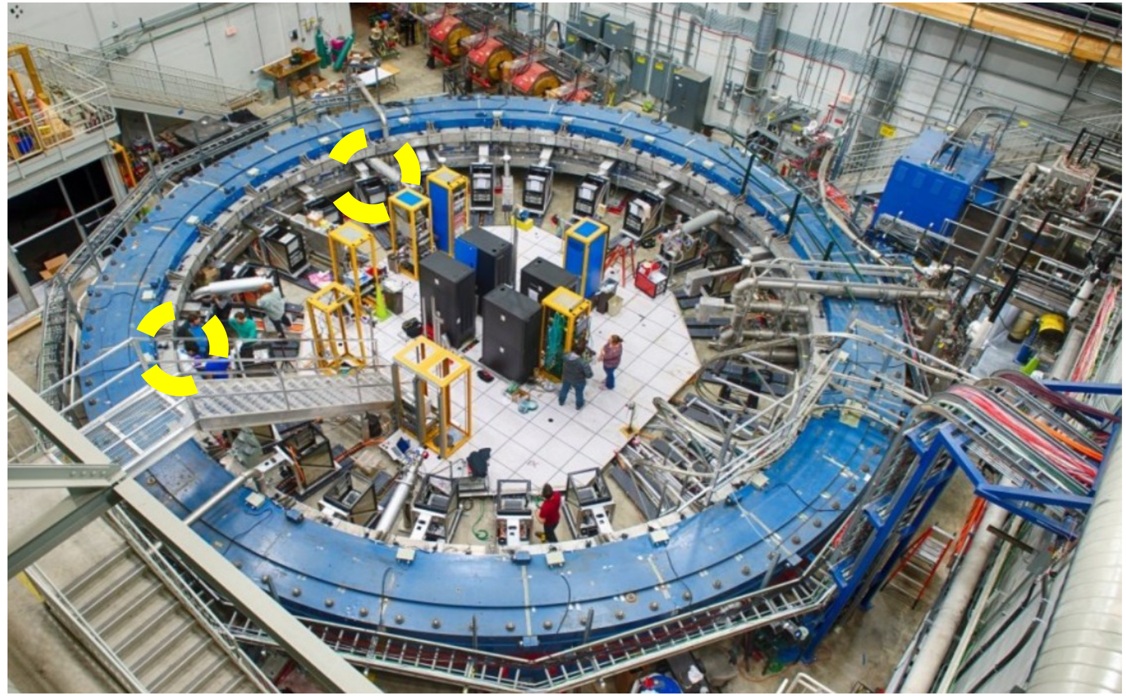

- Tracker data used to construct beam profiles
- Resolution ~100 μm

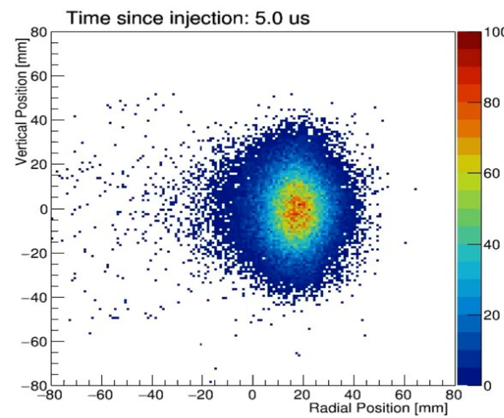

Muon Spin Precession

- In a purely transverse magnetic field, spin precession frequency

$$\overrightarrow{\omega_s} = -\frac{ge\overrightarrow{B}}{2m_\mu} - (1-\gamma)\frac{e\overrightarrow{B}}{m_\mu\gamma}$$

- Cyclotron frequency

$$\overrightarrow{\omega_c} = \frac{e\overrightarrow{B}}{2m_\mu\gamma}$$

- Difference

$$\overrightarrow{\omega_a} = \overrightarrow{\omega_s} - \overrightarrow{\omega_c} = -(\frac{g-2}{2})\frac{e\overrightarrow{B}}{m_\mu} = -a_\mu\frac{e\overrightarrow{B}}{m_\mu}$$

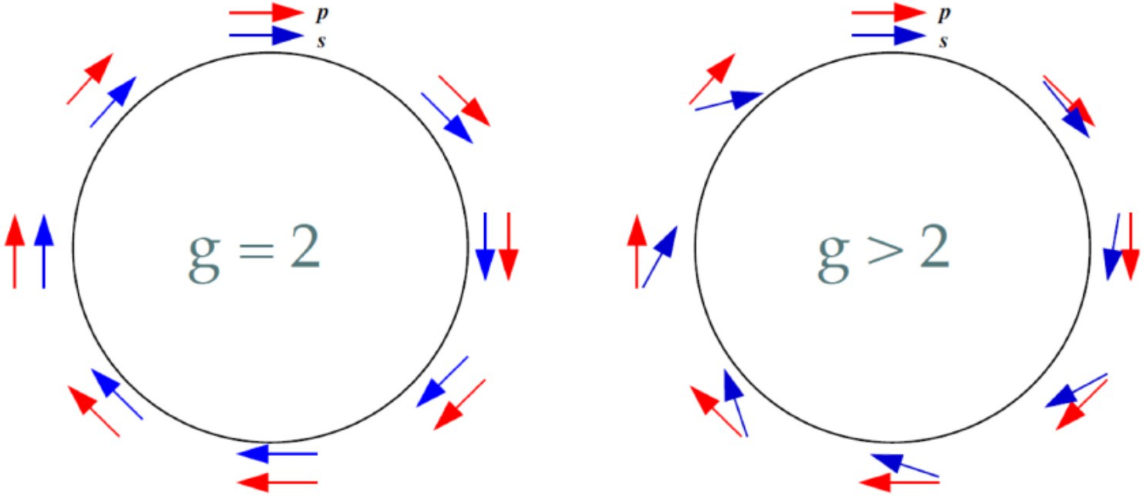

Muon Spin Precession

- Since our setup also has a quadrupole electric field

$$\vec{\omega}_a = -\frac{e}{m_\mu}[a_\mu \vec{B} - (a_\mu - \frac{1}{\gamma^2 - 1})\frac{\vec{\beta} \times \vec{E}}{c}]$$

- But we can choose γ such that

$$\gamma = \sqrt{1 + \frac{1}{a_\mu}} \approx 29.3$$

"magic momentum"
3.09 GeV/c

- So we only need to measure $\vec{\omega}_a$ and $\vec{B}$ experimentally

$$\omega_a = -a_\mu \frac{e\vec{B}}{m_\mu}$$

Magnetic field measurement

- Pulsed proton NMR
- 378 NMR probes azimuthally distributed around the ring
- 17 trolley (movable) NMR probes
  ~ run every 3 days during data taking

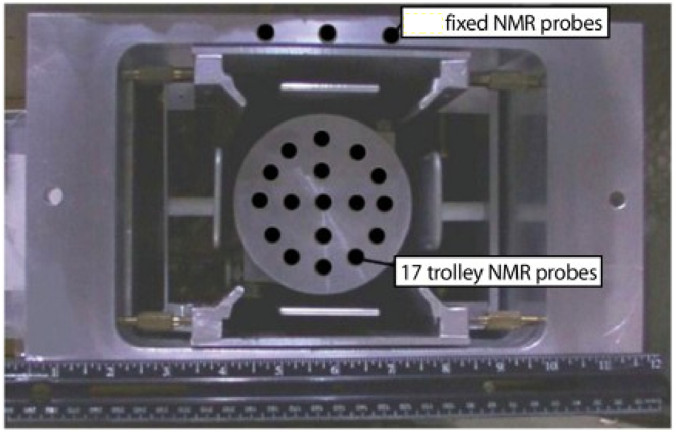

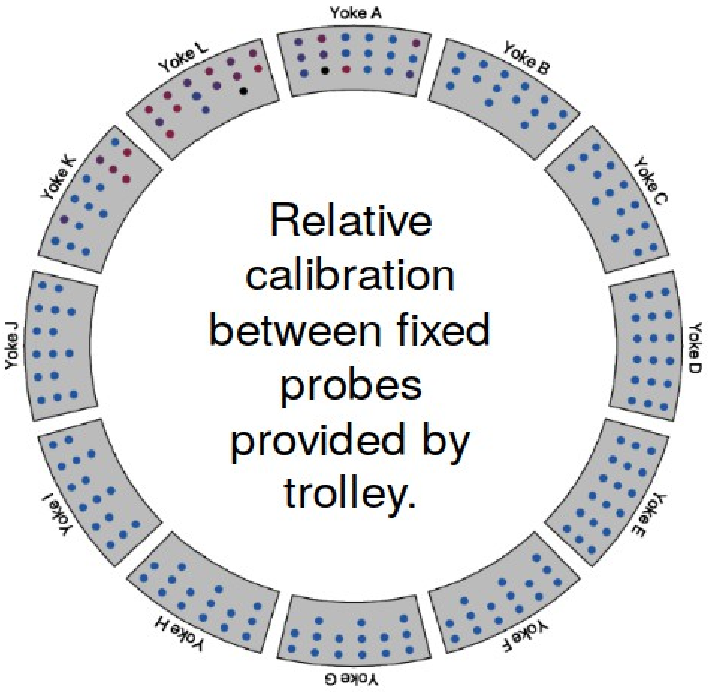

Magnetic field measurement

- Precession frequency of proton related to B-field

$$\hbar\omega'_p = 2\mu_p B$$

- After some rearrangement and using $e = \dfrac{4m_e\mu_e}{\hbar g_e}$

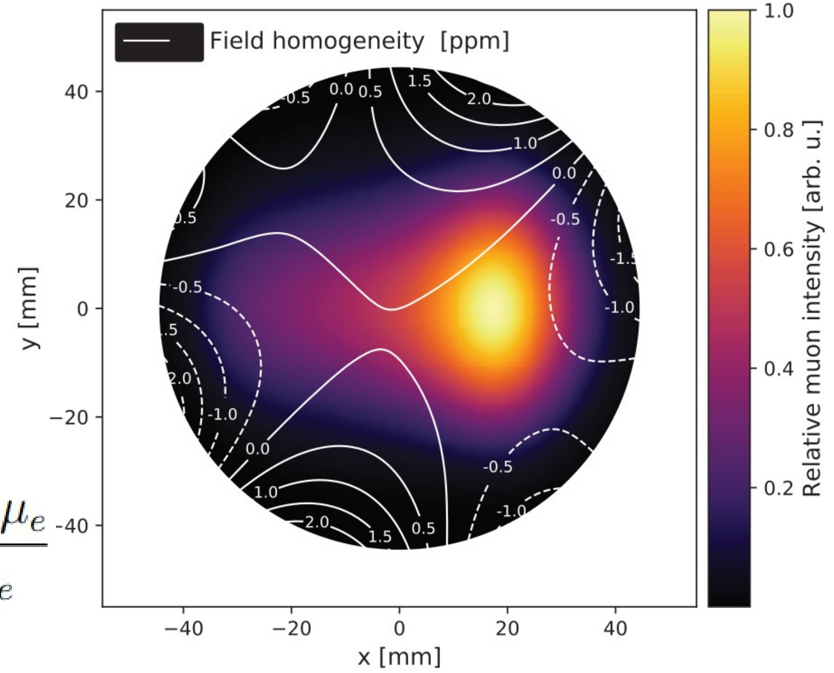

$$a_\mu = \boxed{\frac{\omega_a}{\tilde{\omega}_p}} \frac{m_\mu}{\underbrace{m_e}_{22\text{ ppb}}} \frac{\mu_p}{\underbrace{\mu_e}_{3\text{ ppb}}} \frac{g_e}{\underbrace{2}_{0.26\text{ ppt}}}$$

- All other quantities are measured experimentally with high precision

ω_a measurement

Muon decays into positrons → violates parity $\mu^+ \rightarrow e^+ + \nu_\mu + \overline{\nu_e}$

- In muon rest frame

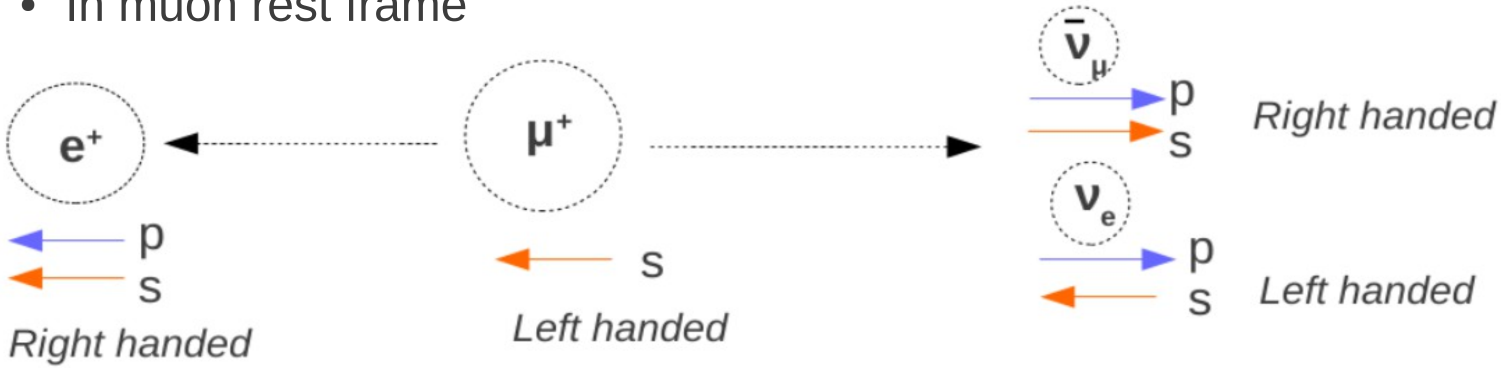

Highest energy decay configuration

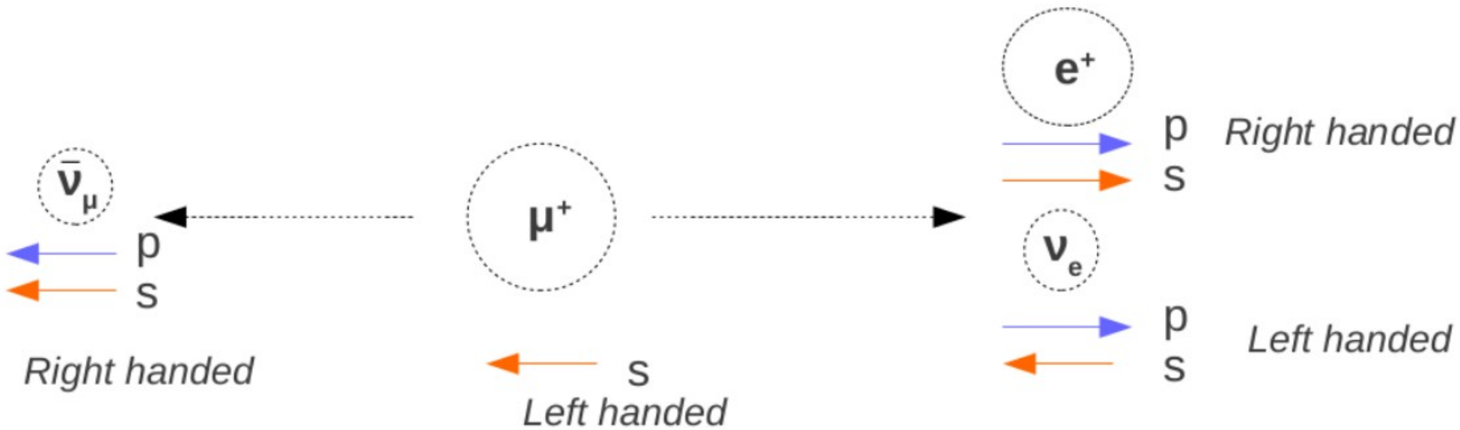

Lowest energy decay configuration

ω_a measurement

- In lab frame number of high energy positrons oscillates with ω_a
- Similarly, total energy of the positrons also oscillates with ω_a

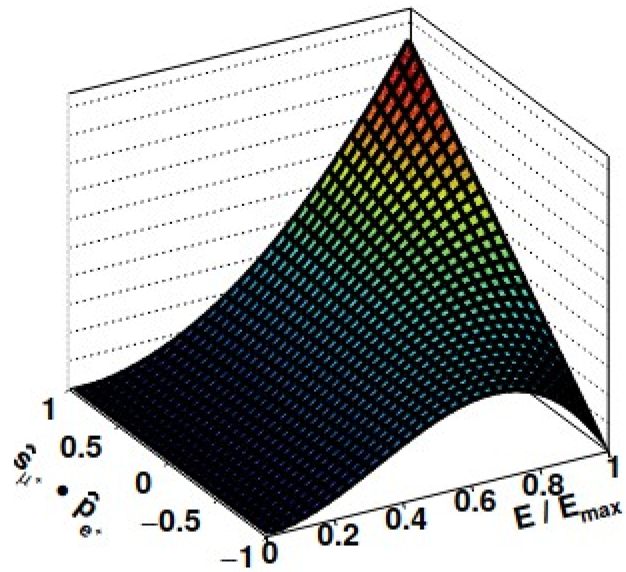

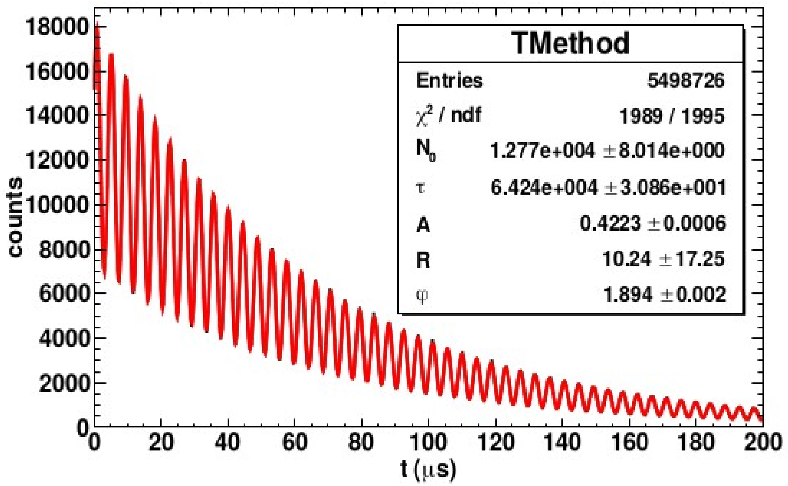

Threshold or T-method

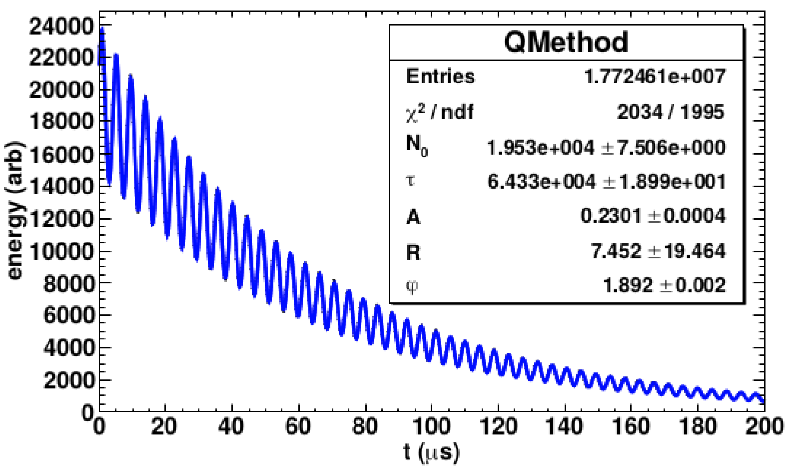

Energy Integrating or Q-method

ω_a analysis

- Contstruct *energy vs time* or *high energy positron count vs time* histograms
- Fit histograms with appropriate function
- Most precise histogram is asymmetry weighted (A-method)

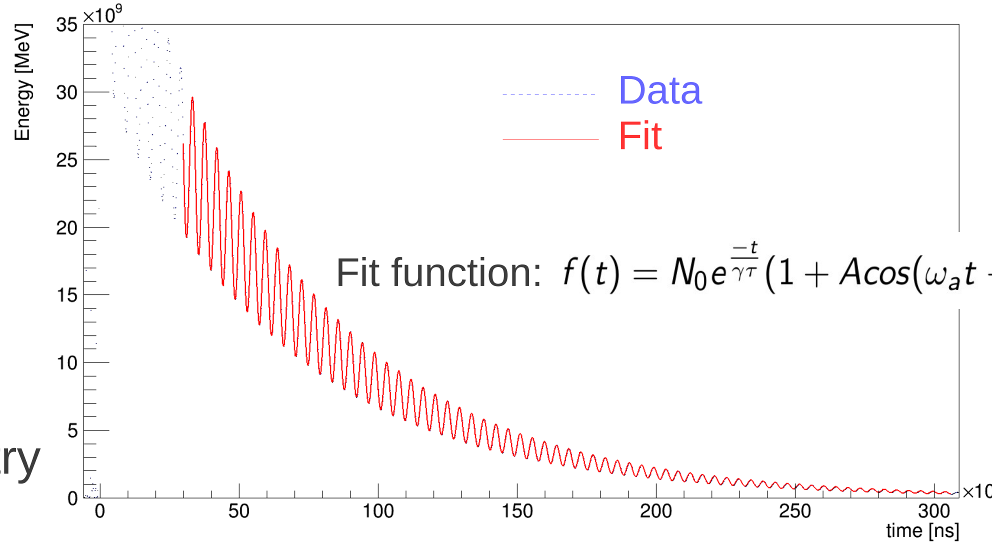

Fit function: $f(t) = N_0 e^{\frac{-t}{\gamma\tau}}(1 + A\cos(\omega_a t - \phi))$

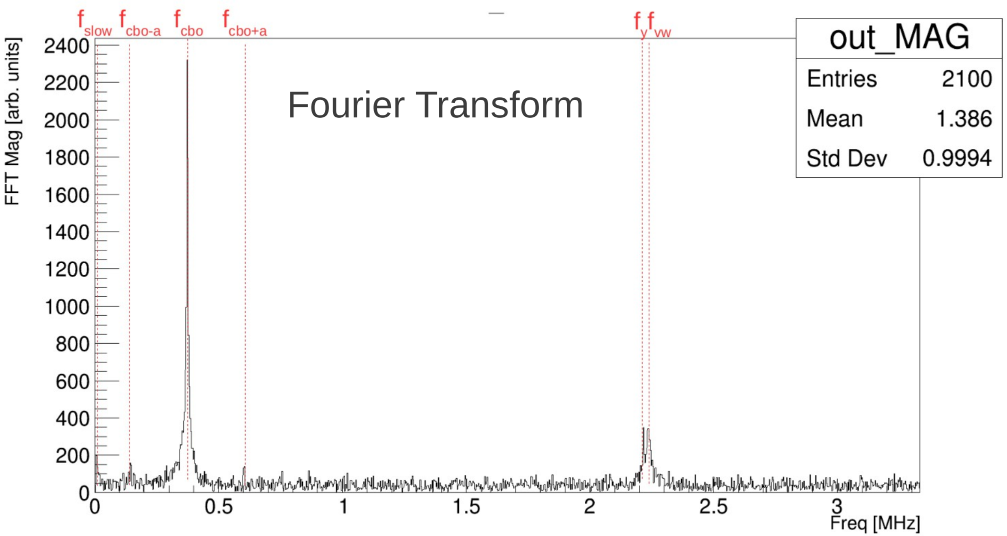

Correct fit function:

$$f(t) = N_0 N_{CBO}(t) N_{VW}(t) N_y(t) \Lambda(t) e^{\frac{-t}{\tau}} (1 + A_0 A(t) cos(\omega_a t - \phi_0 - \phi(t)))$$

where

$$N_{CBO}(t) = 1 + A_{CBO_N} e^{\frac{-t}{\tau_{CBO}}} cos(\omega_{CBO} t - \phi_{CBO_N}) + A_{2CBO_N} e^{\frac{-2t}{\tau_{CBO}}} cos(2\omega_{CBO} t - \phi_{2CBO_N})$$

$$N_{VW}(t) = 1 + A_{vw} e^{\frac{-t}{\tau_{VW}}} cos(\omega_{VW} t - \phi_{VW})$$

$$N_y(t) = 1 + A_y e^{\frac{-t}{\tau_y}} cos(\omega_y t - \phi_y)$$

$$A(t) = 1 + A_{CBO_A} e^{\frac{-t}{\tau_{CBO}}} cos(\omega_{CBO} t - \phi_{CBO_A})$$

$$\phi(t) = A_{CBO_\phi} e^{\frac{-t}{\tau_{CBO}}} cos(\omega_{CBO} t - \phi_{CBO_\phi})$$

$$\Lambda(t) = 1 - \kappa_{loss} \int_0^t L(t') e^{\frac{t'}{\tau}} dt'$$

Final Measurement

Frequency of the clock recording time

Muon precession frequency

E-field correction

Pitch correction

Muon loss

Phase acceptance

$$\mathcal{R}'_\mu \approx \frac{f_{\mathrm{clock}}\,\omega_a^m (1 + C_e + C_p + C_{ml} + C_{pa})}{f_{\mathrm{calib}} \langle \omega_p(x,y,\phi) \times M(x,y,\phi) \rangle (1 + B_k + B_q)}$$

Calibration factor of NMR probes

Proton precession frequency (B-field)

Muon population distribution

Transient fields

Clock Blinding

- The master clock is 40MHz
- Blinded by detuning to a secret value between 39 997 to 39 999 kHz
- Only two people outside of the collaboration know the exact value
- Unblinding only after all the analysis is frozen

$$\mathcal{R}'_\mu \approx \frac{f_{\text{clock}}\,\omega_a^m\,(1 + C_e + C_p + C_{ml} + C_{pa})}{f_{\text{calib}}\,\langle \omega_p(x,y,\phi) \times M(x,y,\phi) \rangle\,(1 + B_k + B_q)}$$

Frequency of the clock recording time

Muon precession frequency

E-field correction

Pitch correction

Muon loss

Phase acceptance

Calibration factor of NMR probes

Proton precession frequency (B-field)

Muon population distribution

Transient fields

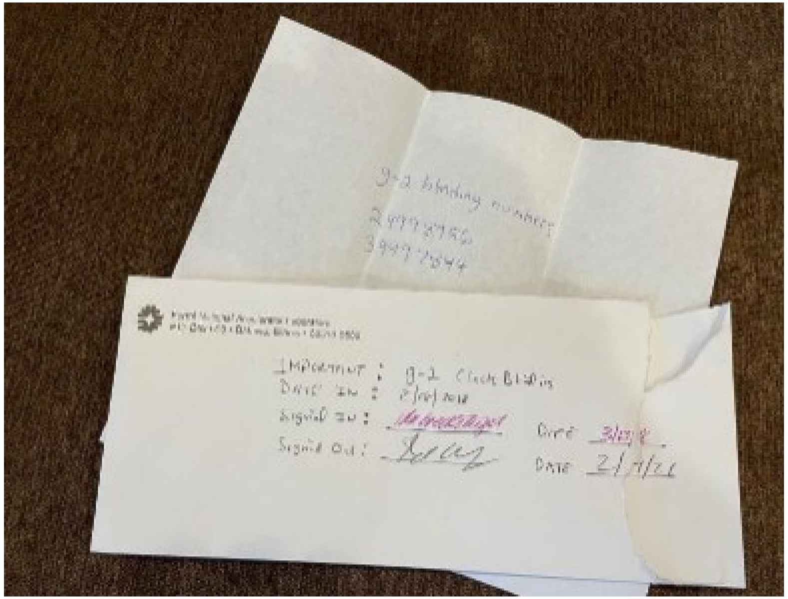

Run 1 secret values revealed during unblinding

E-field correction

- In the experimental setup, there is a spread in muon momentum

- All muons are not located at the center where radial electric field is zero.

Frequency of the clock recording time
Muon precession frequency
E-field correction
Pitch correction
Muon loss
Phase acceptance

$$\mathcal{R}'_\mu \approx \frac{f_{\text{clock}}\,\omega_a^m(1+C_e+C_p+C_{ml}+C_{pa})}{f_{\text{calib}}\langle\omega_p(x,y,\phi)\times M(x,y,\phi)\rangle(1+B_k+B_q)}$$

Calibration factor of NMR probes
Proton precession frequency (B-field)
Muon population distribution
Transient fields

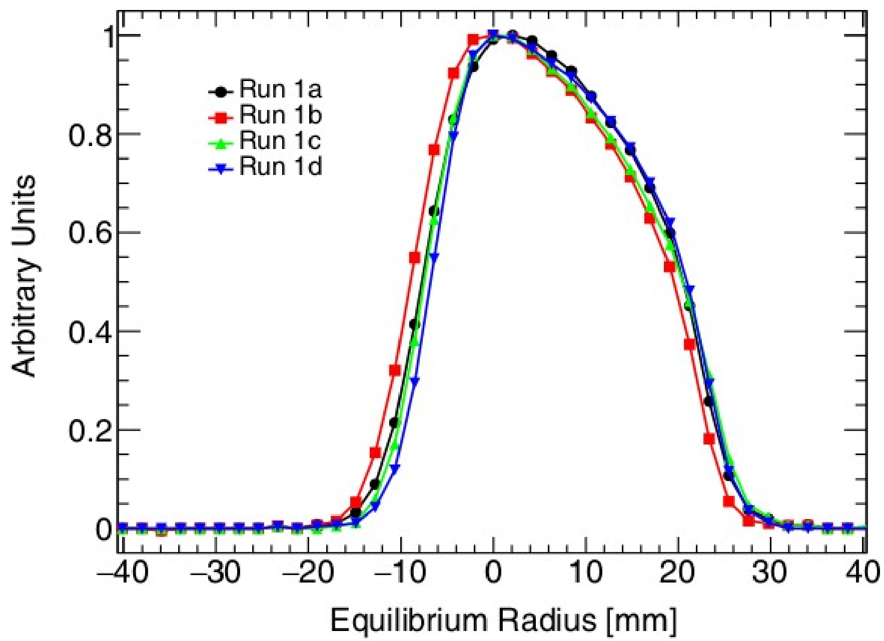

- There is a correction to ω_a in the vertical direction

$$C_e \approx 2n(1-n)\beta_0^2\frac{\langle x_e^2\rangle}{R_0^2}$$

- Run-1 correction: 489 ppb
  uncertainty: 53 ppb

Pitch Correction

- The condition $\vec{\beta} . \vec{B} = 0$ is not satisfied due to the vertical beam oscillation in quadrupole E-field

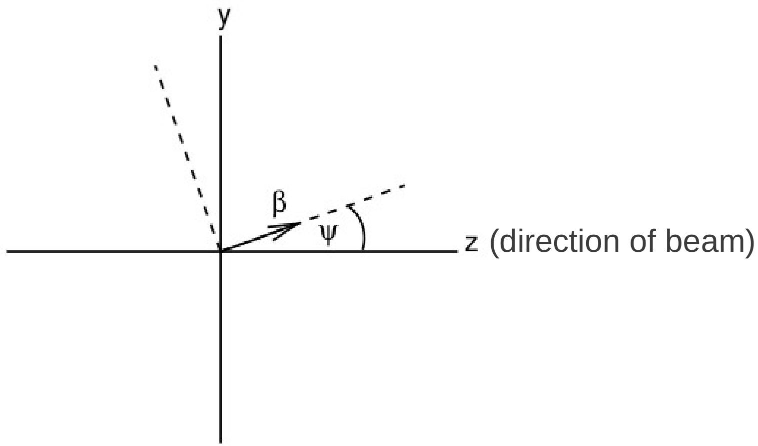

Frequency of the clock recording time
Muon precession frequency
E-field correction
Pitch correction
Muon loss
Phase acceptance

$$\mathcal{R}'_\mu \approx \frac{f_{\mathrm{clock}}\,\omega_a^m (1 + C_e + \boxed{C_p} + C_{ml} + C_{pa})}{f_{\mathrm{calib}} \langle \omega_p(x,y,\phi) \times M(x,y,\phi) \rangle (1 + B_k + B_q)}$$

Calibration factor of NMR probes
Proton precession frequency (B-field)
Muon population distribution
Transient fields

- Correction applied

$$C_p \approx \frac{n}{2}\frac{\langle y^2 \rangle}{R_0^2} = \frac{n}{4}\frac{\langle A^2 \rangle}{R_0^2}$$

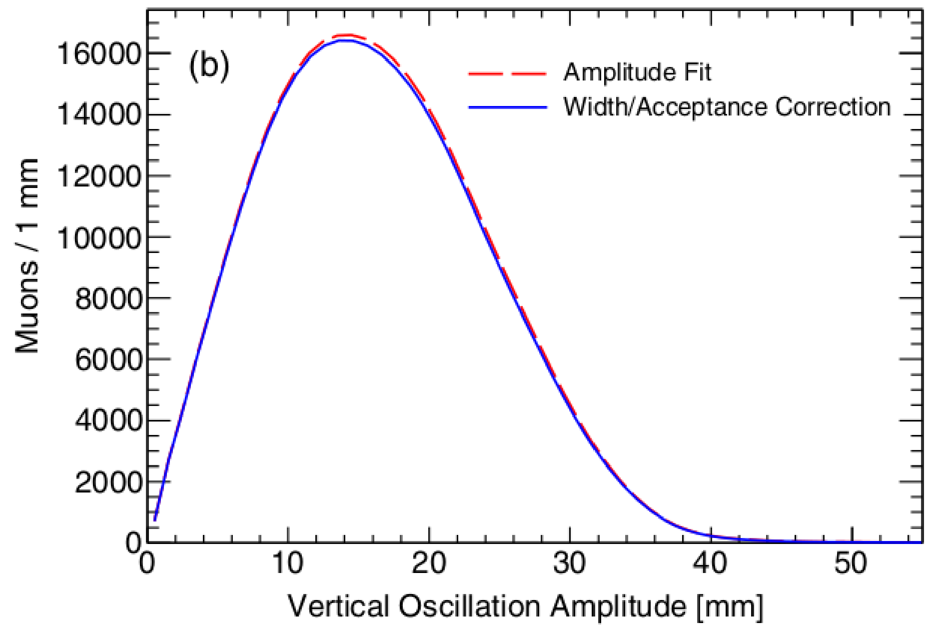

- Run 1 correction: 180 ppb
  uncertainty: 13 ppb

Lost muons

- Some muons are lost from the storage region
- Pass through the detectors as MIPs

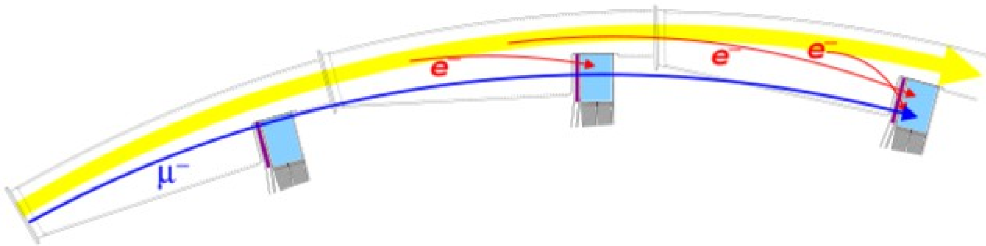

- Changes ω_a phase:

$$\frac{d\langle\phi\rangle}{d\langle p\rangle}\cdot\frac{d\langle p\rangle}{dt}=\frac{d\langle\phi\rangle}{dt}=\Delta\omega_a\neq 0$$

- Time dependent (early-to-late effect)
- Run 1 correction: 11 ppb
  uncertainty: 5 ppb

Frequency of the clock recording time
Muon precession frequency
E-field correction
Pitch correction
$\boxed{\text{Muon loss}}$
Phase acceptance

$$\mathcal{R}'_\mu \approx \frac{f_{\rm clock}\,\omega_a^m(1+C_e+C_p+C_{ml}+C_{pa})}{f_{\rm calib}\langle\omega_p(x,y,\phi)\times M(x,y,\phi)\rangle(1+B_k+B_q)}$$

Calibration factor of NMR probes
Proton precession frequency (B-field)
Muon population distribution
Transient fields

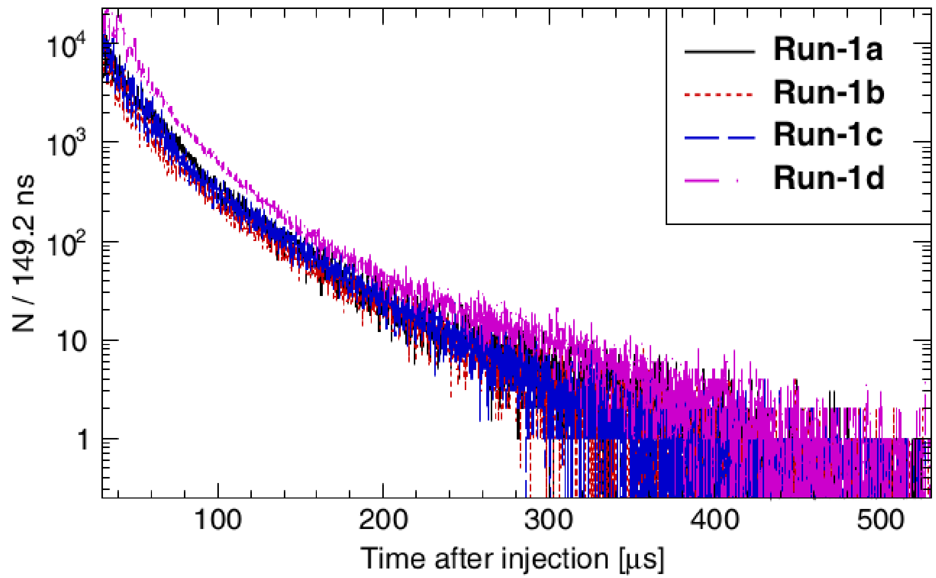

Phase acceptance

Frequency of the clock recording time
Muon precession frequency
E-field correction
Pitch correction
Muon loss
$\boxed{\text{Phase acceptance}}$

$$\mathcal{R}'_\mu \approx \frac{f_{\text{clock}}\,\omega_a^m (1 + C_e + C_p + C_{ml} + C_{pa})}{f_{\text{calib}}\langle \omega_p(x,y,\phi) \times M(x,y,\phi)\rangle (1 + B_k + B_q)}$$

Calibration factor of NMR probes
Proton precession frequency (B-field)
Muon population distribution
Transient fields

- Two damaged resistors discovered after Run-1
- Beam was moving vertically during measurement

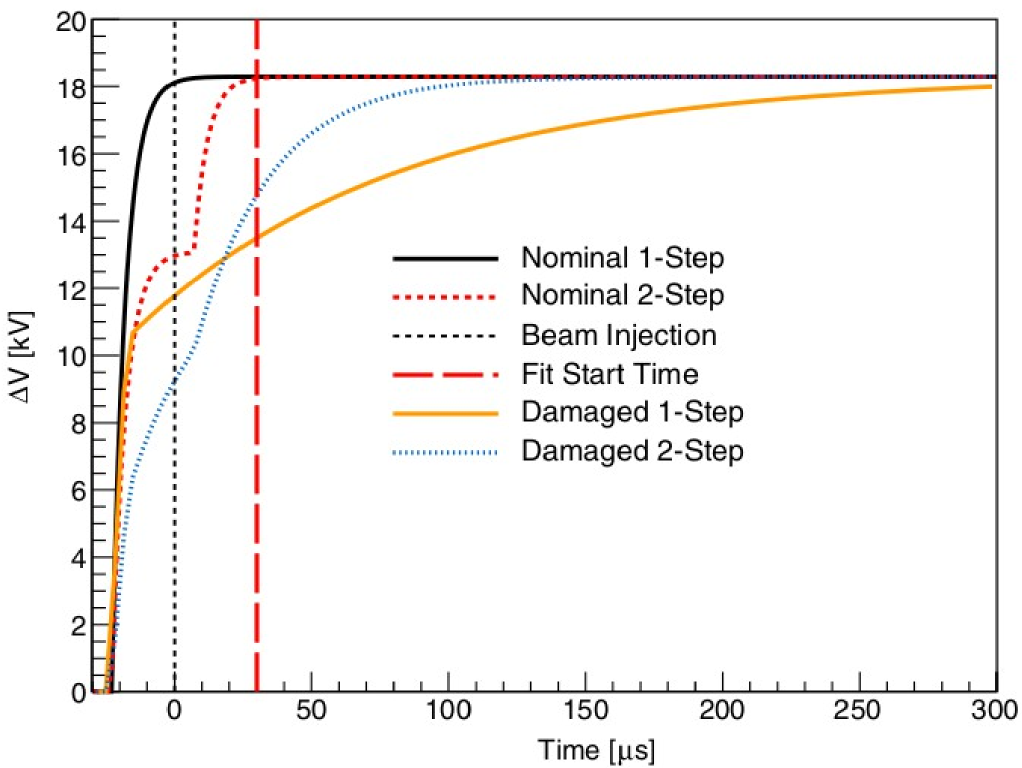

- Calorimeter acceptance affected by decay position
- Phase is correlated to the orientation of muon spin maximizing acceptance
- Time varying phase
- Run-1 correction : 158 ppb
  uncertainty : 75 ppb

Calibration of NMR probes

- Trolley NMR probes are calibrated using a probe containing pure water sample
- Corrected for temperature, material effects and field variations

Frequency of the clock recording time | Muon precession frequency | E-field correction | Pitch correction | Muon loss | Phase acceptance

$$\mathcal{R}'_\mu \approx \frac{f_{\text{clock}}\,\omega_a^m (1 + C_e + C_p + C_{ml} + C_{pa})}{f_{\text{calib}}\langle \omega_p(x,y,\phi) \times M(x,y,\phi)\rangle (1 + B_k + B_q)}$$

Calibration factor of NMR probes | Proton precession frequency (B-field) | Muon population distribution | Transient fields

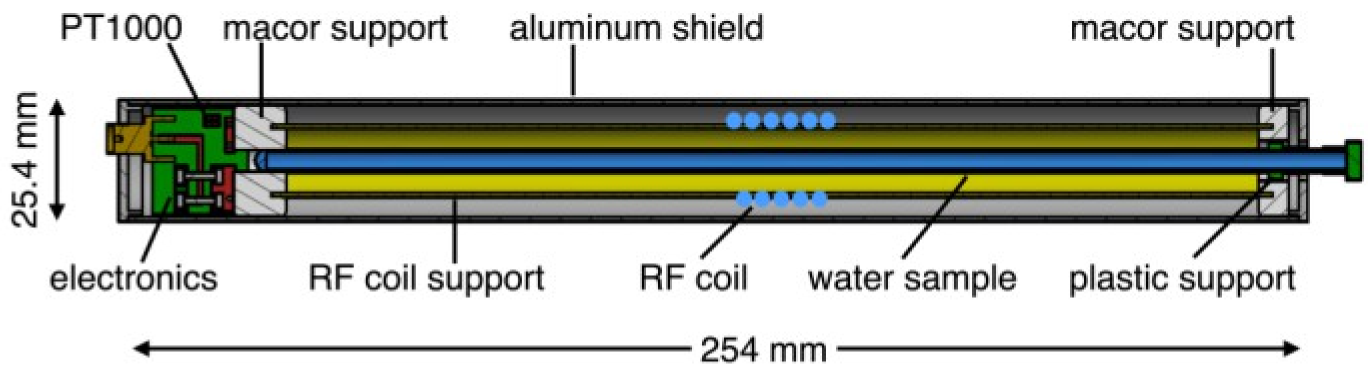

- Uncertainty on Run 1 calibrations less than 20 ppb

Muon population distribution

Frequency of the clock recording time; Muon precession frequency; E-field correction; Pitch correction; Muon loss; Phase acceptance

$$\mathcal{R}'_\mu \approx \frac{f_{\text{clock}}\,\omega_a^m(1+C_e+C_p+C_{ml}+C_{pa})}{f_{\text{calib}}\langle\omega_p(x,y,\phi)\times M(x,y,\phi)\rangle(1+B_k+B_q)}$$

Calibration factor of NMR probes; Proton precession frequency (B-field); Muon population distribution; Transient fields

- ω_p measured by NMR probes have to be weighted by muon distribution
- The spatial and temporal muon population distribution is averaged over

$$\tilde{\omega}'_p = \frac{\int_0^T dt \int_0^{2\pi} d\phi \int_{r_1}^{r_2} dr \int_{-y_0}^{y_0} dy\, r\,\rho^\mu(r,y,\phi,t)\,\omega'_p(r,y,\phi,t)}{\int_0^T dt \int_0^{2\pi} d\phi \int_{r_1}^{r_2} dr \int_{-y_0}^{y_0} dy\, r\,\rho^\mu(r,y,\phi,t)}$$

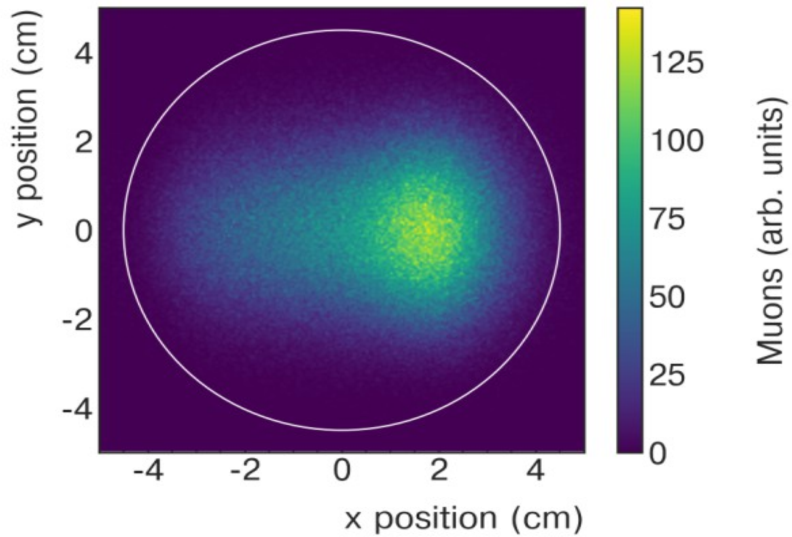

Transient fields

- Magnetic field measurement insensitive to perturbation due to kicker eddy current → **B_k**
- Also do not pick up transient field due to mechanical vibration of ESQ → **B_q**

Frequency of the clock recording time
Muon precession frequency
E-field correction
Pitch correction
Muon loss
Phase acceptance

$$\mathcal{R}'_\mu \approx \frac{f_{\text{clock}}\,\omega_a^m(1+C_e+C_p+C_{ml}+C_{pa})}{f_{\text{calib}}\langle\omega_p(x,y,\phi)\times M(x,y,\phi)\rangle(1+B_k+B_q)}$$

Calibration factor of NMR probes
Proton precession frequency (B-field)
Muon population distribution
Transient fields

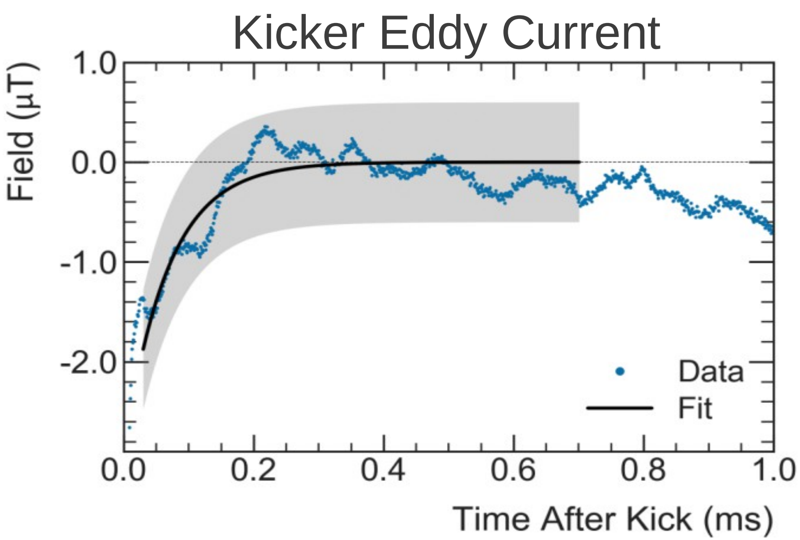

Correction: 27 ppb
Uncertainty: 37 ppb

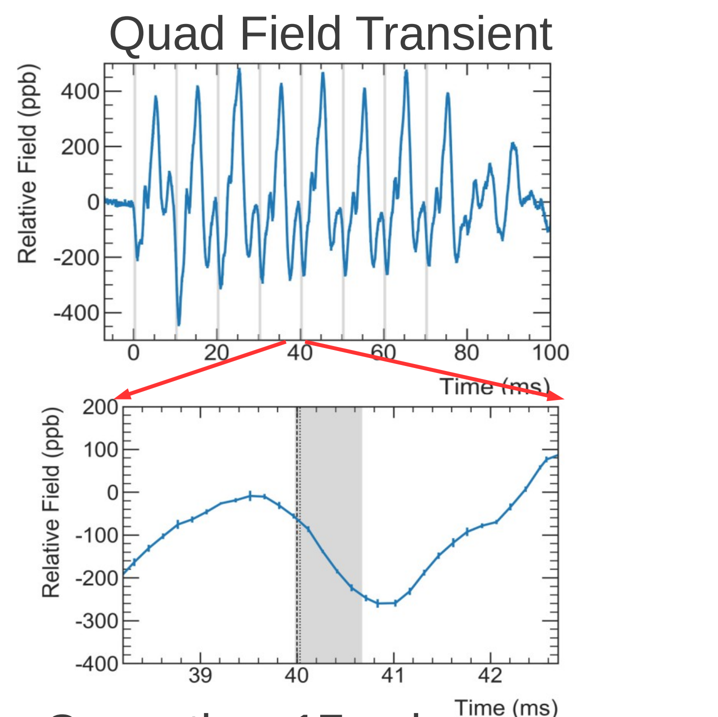

Correction: 17 ppb
Uncertainty: 92 ppb

Run-1 Results

- During analysis all results were blinded
- Two types of blinding in ω_a analysis

  -Hardware blinding of clock frequency

  -Software blinding according to $\omega_a = \omega_{ref}[1 - (R - \Delta R) \times 10^{-6}]$

  where $\omega_{ref} = 2\pi \times 0.2291$ MHz

- There were 6 different analysis for ω_a
- All results in agreement after relative unblinding
- 4 most precise numbers taken for final averaging

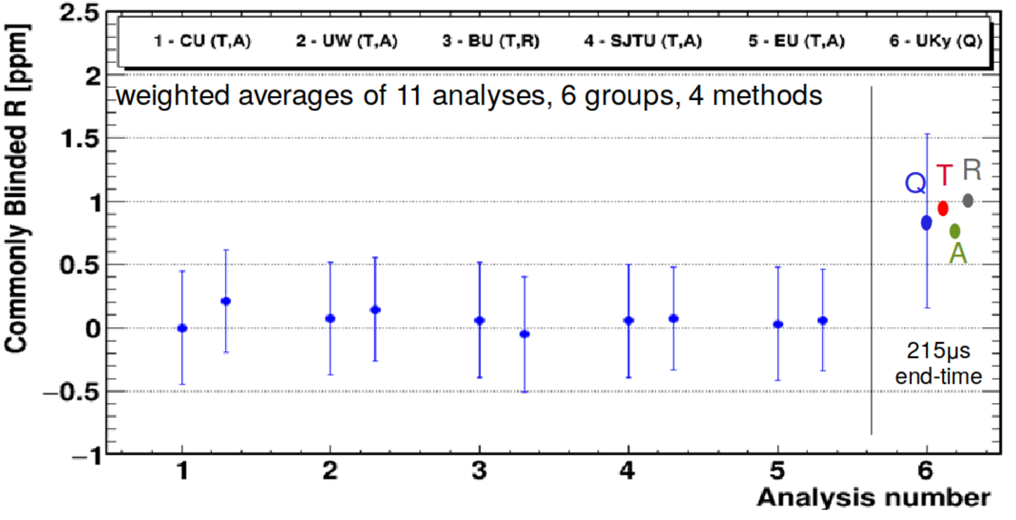

Run-1 Results

- Similarly two parallel analysis for ω_p
- Systematic uncertainty table :

Quantity	Correction terms (ppb)	Uncertainty (ppb)
ω_a^m (statistical)	...	434
ω_a^m (systematic)	...	56
C_e	489	53
C_p	180	13
C_{ml}	−11	5
C_{pa}	−158	75
$f_{\text{calib}} \langle \omega_p(x, y, \phi) \times M(x, y, \phi) \rangle$	...	56
B_k	−27	37
B_q	−17	92
$\mu'_p(34.7°)/\mu_e$	...	10
m_μ/m_e	...	22
$g_e/2$	...	0
Total systematic	...	157
Total fundamental factors	...	25
Totals	544	462

Run-1 Results

- $a_\mu^{FNAL} = 116592040(54) \times 10^{-11}$
- Statistical uncertainty 460 ppb, systematic uncertainty 157 ppb

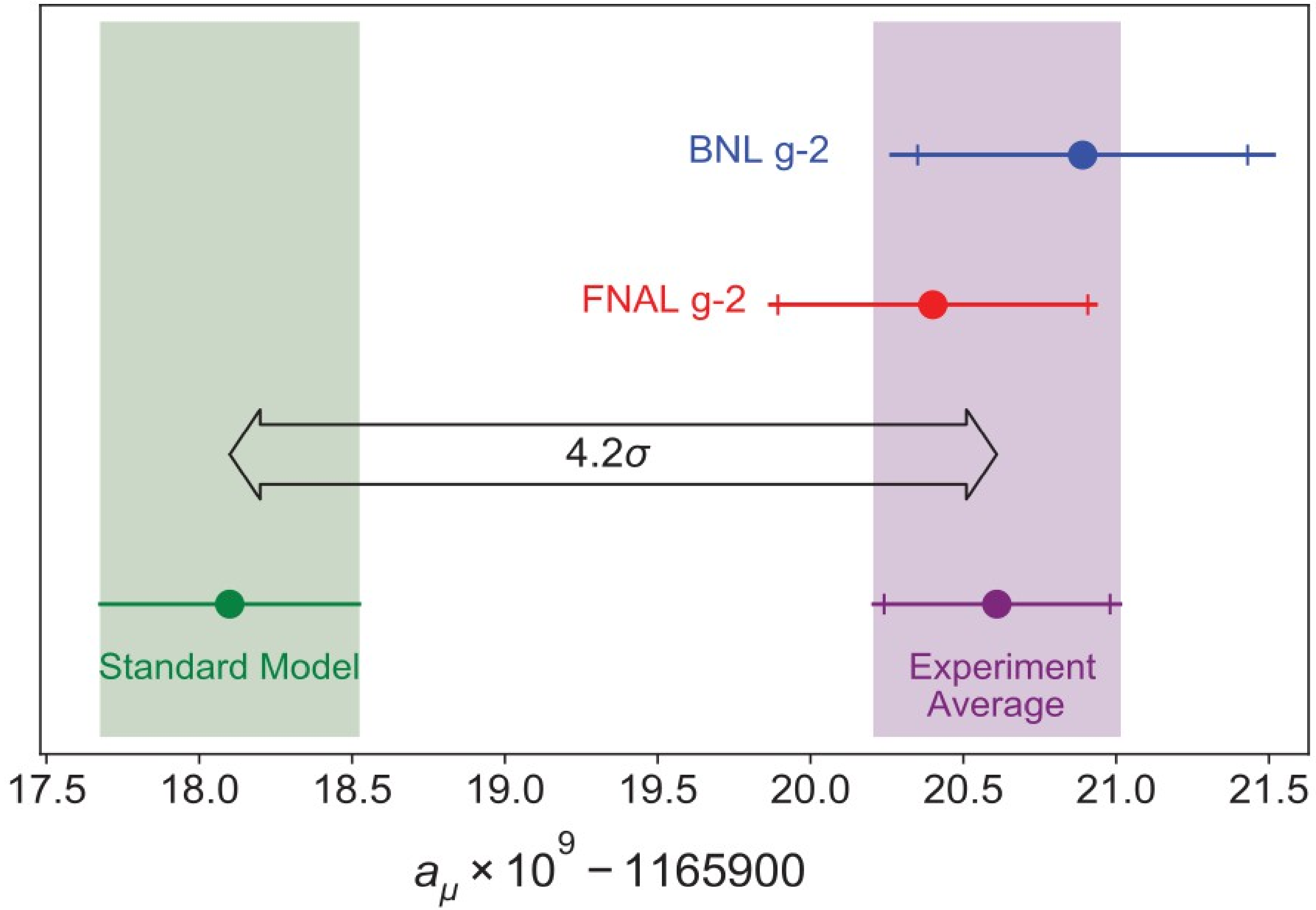

Some Other Developments

- Recent efforts in calculating HVP contribution using Lattice QCD
- Large uncertainty
- BMW collaboration released results in 2021 with much better precision
- Closer to experimental value, disagreement with earlier hadronic contribution cal-culation
- Under review with Muon g-2 Theory Initiative

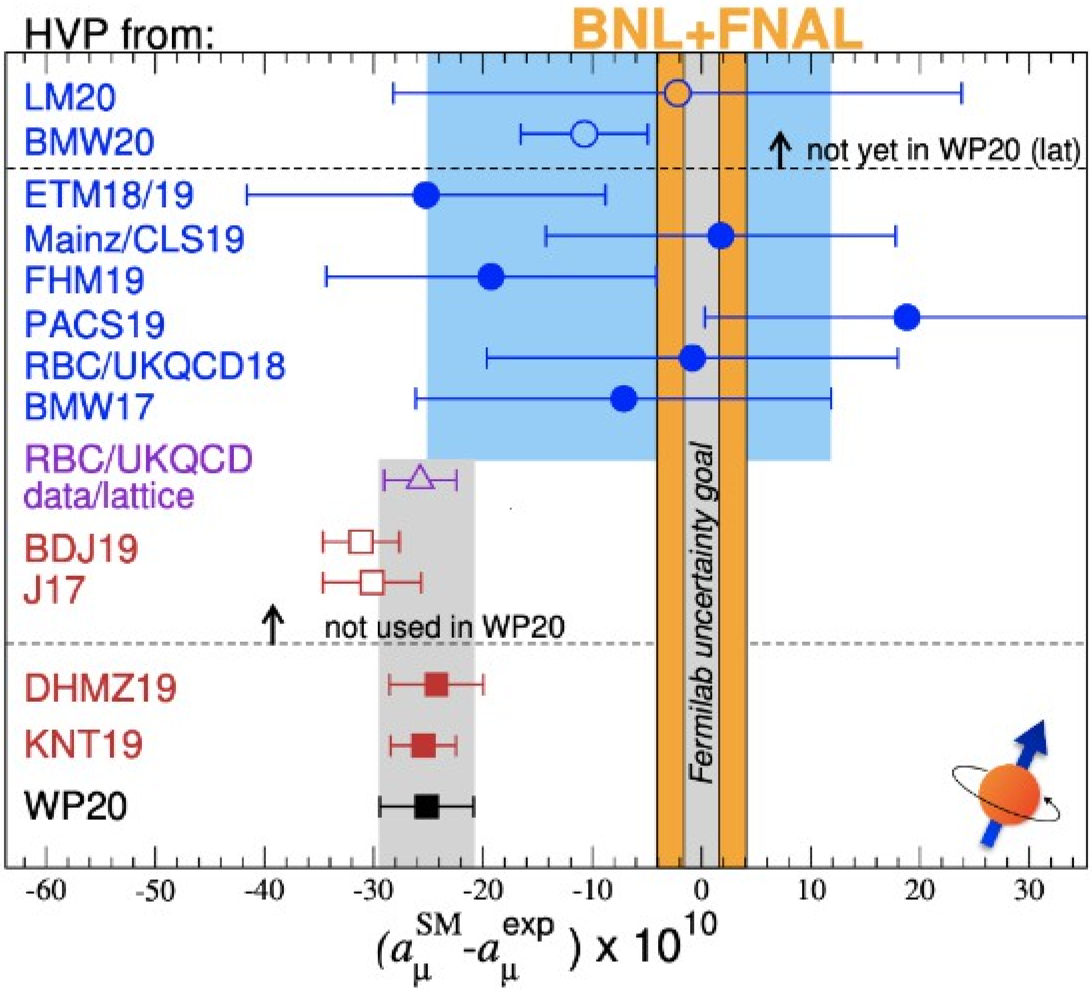

Current status

- Data accumulated so far:

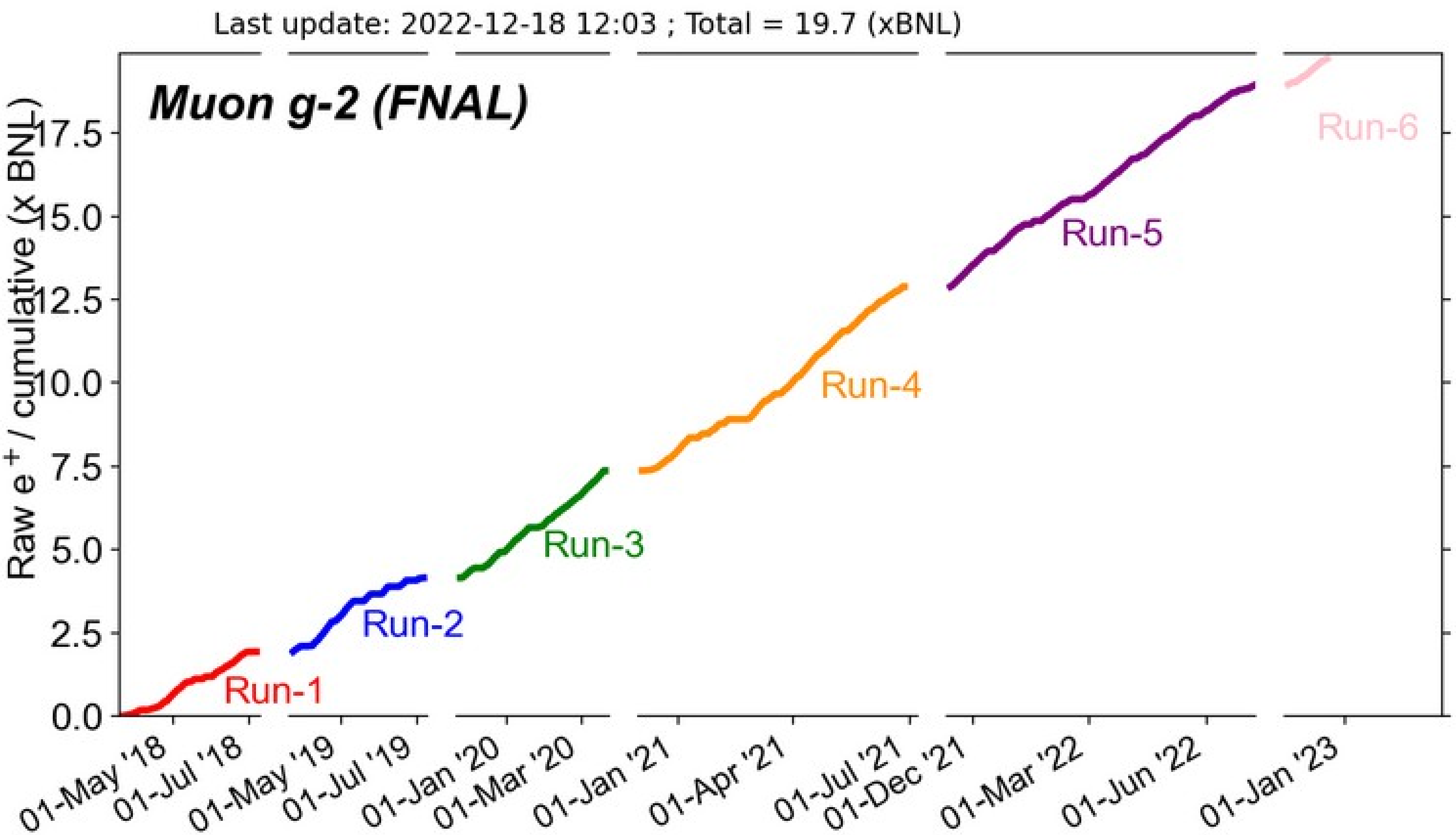

Improvements after Run-1: Fixed broken Quad Resistors

- Run 2+ → broken resistors fixed
- Early time vertical beam motion reduced
- Expected phase acceptance correction reduced

Vertical width variation

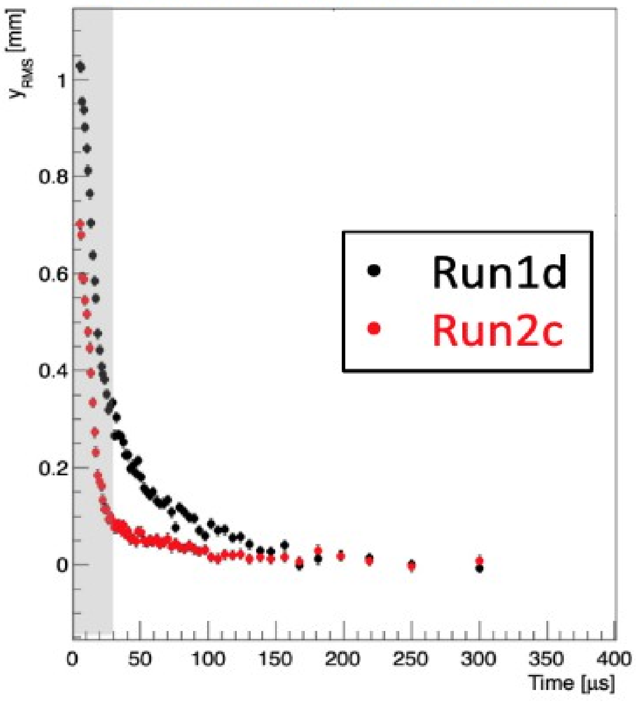

Radial mean variation

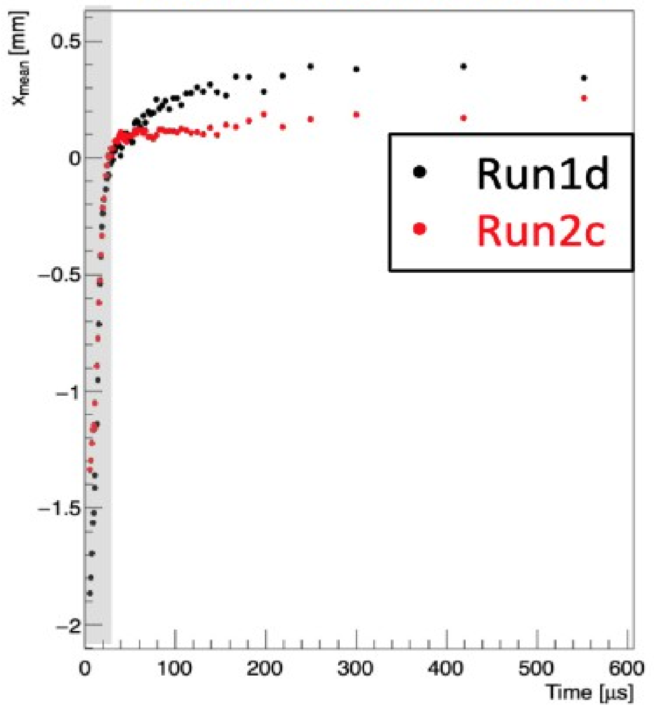

Improvements after Run-1: Improved Kick

- Hardware improvement in the kicker magnet
- Beam more centered in the storage region towards end of Run-3

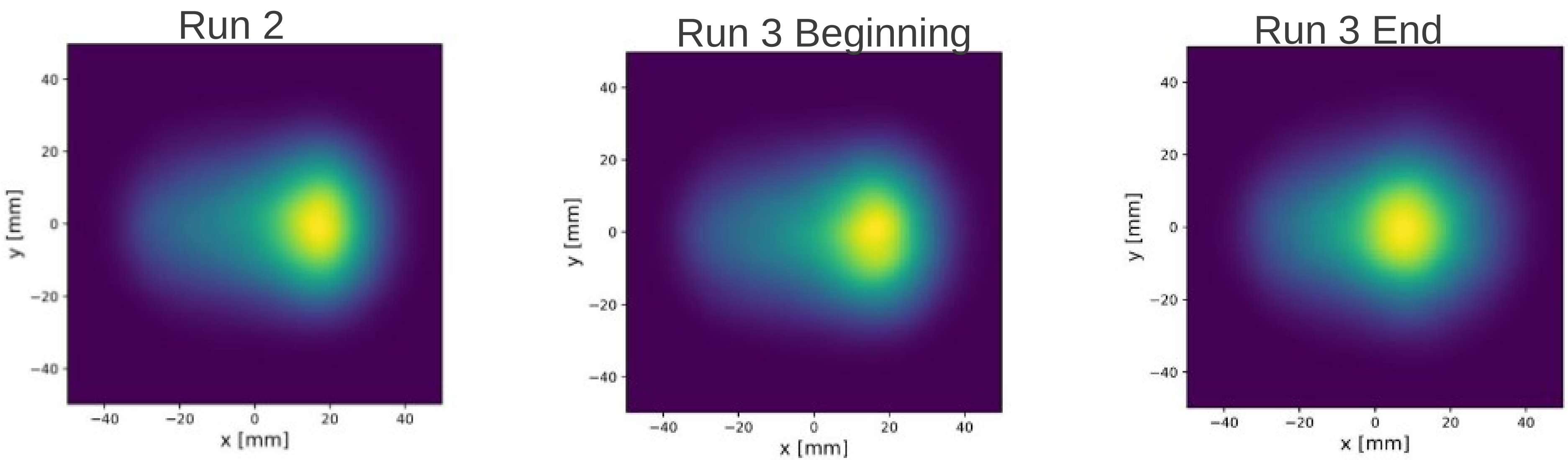

- Reduction in ω_a systematics
- Electric field correction reduced

Improvements after Run-1: Better Temperature Control

- The magnet was better insulated before beginning Run-3
- Experimental hall cooling was improved

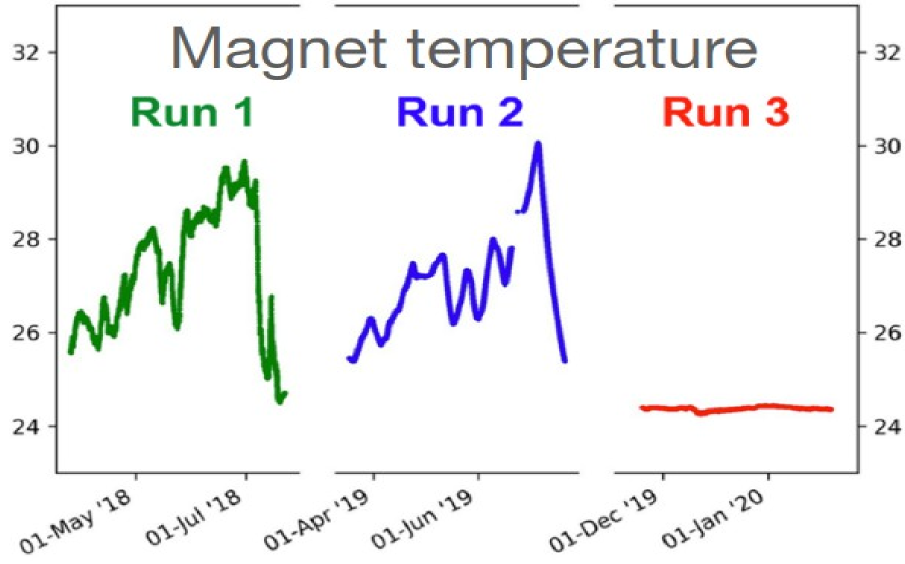

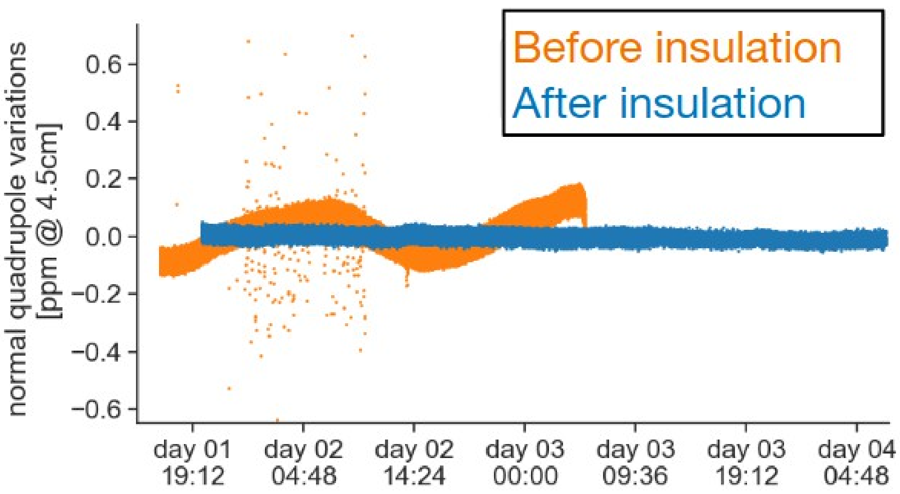

- As a result, better field stability was achieved
- SiPM gain changes were reduced

Improvements after Run-1: ω_a analysis tools

Threshold Method

- Improvement in pile-up procedure

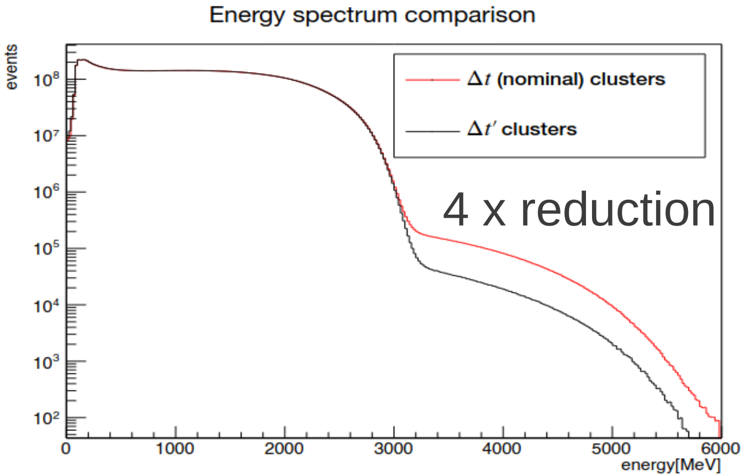

- Improvement in reconstruction techniques
- Efficient histogramming techniques

Energy Integrating Method

- Finer binning for data taking
- Extension of end-time
- Implementation of histogramming techniques to control slow effect systematics

$\boxed{v_1 = v_2 = N(t)}$ $\boxed{u_- = N(t - \frac{T_a}{2})}$, $\boxed{u_+ = N(t + \frac{T_a}{2})}$

$\boxed{V = v_1 + v_2}$ and $\boxed{U = u_+ + u_-}$

$$R = \frac{V-U}{V+U} = \frac{\text{(V - U)}}{\text{(V + U)}} = \text{(h\_ratio)}$$

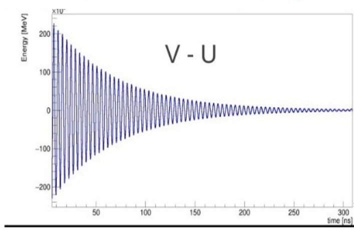

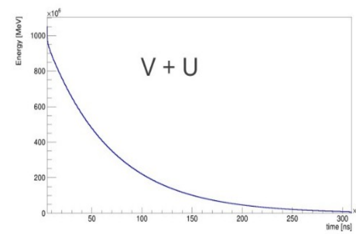

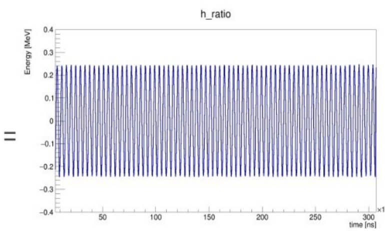

10 x reduction

Current status

- Next release next year, Run 2+3 combined
- Projected statistical uncertainty to be ~200 ppb, factor of 2 improvement over Run 1
- Central analysis complete, values still blinded
- Currently Run-6 data is being recorded
- A total of ~20 times BNL data collected so far
- Expected final precision 140 ppb
- Stay tuned!

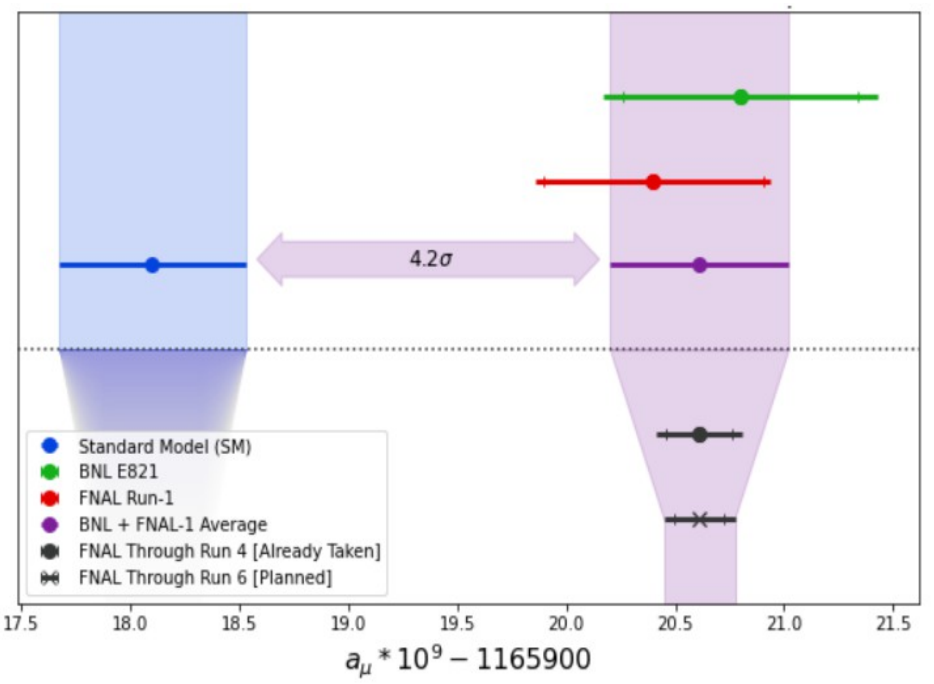

Extra

QED calculation

Magentic moment: $\vec{\mu} = -\frac{e}{2m} g \vec{S}$: $\quad g = 2$ (Dirac) $\quad \Rightarrow$ bare (no quantum effects)

$\Rightarrow$ Renormalise the QED vertex: $\quad \Gamma^{\mu}_{\rm phys}(k_1, k_2) =$

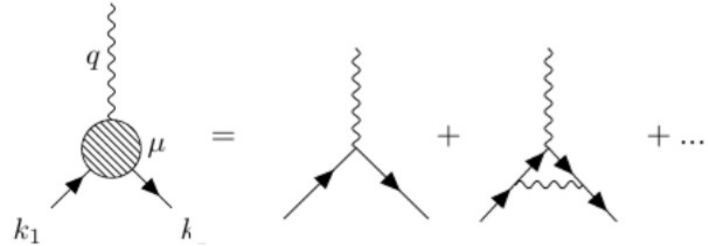

$\Rightarrow$ By virtue of Gordon decomposition: $\Gamma^{\mu}(k_1, k_2) = -ie\left[\gamma^{\mu} F_1(q^2) + \frac{i\sigma^{\mu\nu} q_{\nu}}{2m} F_2(q^2)\right]$

$\Rightarrow$ In NR limit, with $k_2 - k_1 = q \to 0$: $\left(\gamma^{\mu}(\partial_{\mu} - ieA_{\mu}) - m + \frac{eF_2(0)}{4m} F_{\mu\nu}\sigma^{\mu\nu}\right)\psi = 0$

$\rightarrow$ New $F_2(0)$ form factor term in Dirac equation from radiative corrections

$\Rightarrow$ Effective Hamiltonian: $H = \left[\frac{1}{2m}(\vec{p} - e\vec{A})^2 + eA^0 + \frac{e}{2m}(1 + F_2(0))\vec{\sigma}.\vec{B}\right]$

$\rightarrow$ Magnetic potential $U = -\vec{\mu} \cdot \vec{B} = \frac{e}{2m}(1 + F_2(0))\vec{\sigma}.\vec{B} = \frac{e}{2m} g \vec{S}.\vec{B} = \frac{e}{4m} g \vec{\sigma}.\vec{B}$

$\Rightarrow$ Implies $g = 2 + 2F_2(0)$ with quantum effects $\longrightarrow a = F_2(0) = (g-2)/2$

QED calculation

⇒ Consider the 1-loop correction to the QED vertex:

$$\Gamma^{\mu}_{\text{1-loop}}(k_1, k_2) =$$

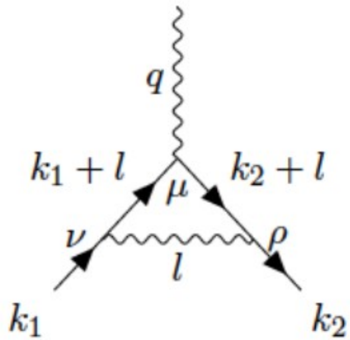

$$= e^3 \int \frac{\mathrm{d}^4 l}{(2\pi)^4} \frac{\gamma^\rho \left(i(\not{k}_2 + \not{l}) + m\right) \gamma^\mu \left(i(\not{k}_1 + \not{l}) + m\right) \gamma^\nu}{\left((k_2 + l)^2 - m^2 - i\varepsilon\right)\left((k_1 + l)^2 - m^2 - i\varepsilon\right)} \frac{g_{\nu\rho}}{(l^2 - i\varepsilon)}$$

⇒ Evaluating the integral and solving for $g - 2$: $\quad a_l^{1-\text{loop}} = F_2^{1-\text{loop}}(0) = \dfrac{e^2}{8\pi^2} = \dfrac{\alpha}{2\pi}$

⇒ The QED contributions have been calculated up to 5-loop order $(\mathcal{O}(\alpha^5))$

$$a_\ell = C_1 \left(\frac{\alpha}{\pi}\right) + C_2 \left(\frac{\alpha}{\pi}\right)^2 + C_3 \left(\frac{\alpha}{\pi}\right)^3 + C_4 \left(\frac{\alpha}{\pi}\right)^4 + C_5 \left(\frac{\alpha}{\pi}\right)^5 + \cdots$$

$$C_L = A_1^{(2L)} + A_2^{(3L)}(m_\ell / m'_\ell) + A_3^{(4L)}(m_\ell / m'_\ell, m_\ell / m''_\ell)$$

Hadronic contribution

$\Rightarrow$ We want to calculate the leading order hadronic vacuum polarisation (HVP) contribution

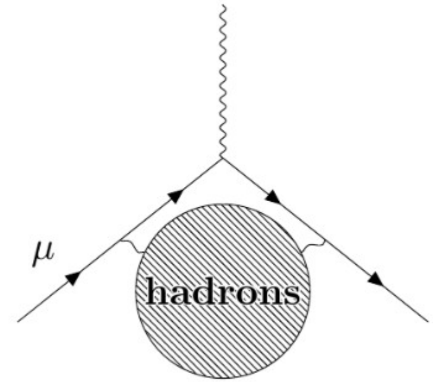

1) Feynman rules for HVP insertion to photon propagator:

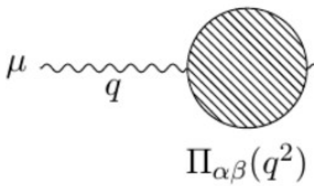

$$= \frac{-ig^{\mu\alpha}}{(q^2 - i\varepsilon)}(-ie)i\Pi_{\alpha\beta}(q^2)(-ie)\frac{-ig^{\beta\nu}}{(q^2 - i\varepsilon)}$$

2) Employ analyticity:

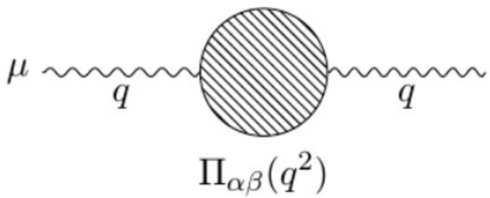

$$= \frac{ie^2 g_{\mu\nu}}{(q^2 - i\varepsilon)^2}\frac{q^4}{\pi}\int_{s_{th}}^{\infty} \mathrm{d}s \frac{\mathrm{Im}\,\Pi(s)}{s(s - q^2 - i\varepsilon)}$$

3) Insert to vertex correction, solve for a_μ: $a_\mu^{\mathrm{had,\,LO\,VP}} = \dfrac{\alpha}{\pi^2}\displaystyle\int_{s_{th}}^{\infty}\frac{\mathrm{d}s}{s}\mathrm{Im}\,\Pi_{\mathrm{had}}(s)K(s)$

4) Utilise optical theorem:

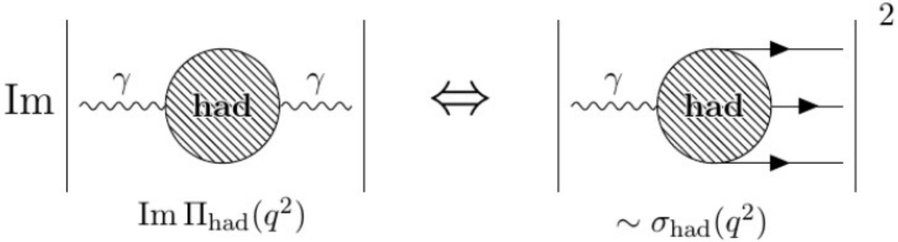

5) Arrive at equation for $a_\mu^{\mathrm{had,\,LO\,VP}}$:

$$a_\mu^{\mathrm{had,\,LO\,VP}} = \frac{1}{4\pi^3}\int_{s_{th}}^{\infty} \mathrm{d}s\, \sigma^0_{\mathrm{had},\gamma}(s)K(s)$$

$\sigma^0_{\mathrm{had},\gamma}$ = bare cross section

Hadronic contribution

$$a_\mu^{\text{had, LO VP}} = \frac{\alpha^2}{3\pi^2}\int_{s_{th}}^{\infty}\frac{\mathrm{d}s}{s}\,R(s)K(s),\ \text{where}\ R(s) = \frac{\sigma^0_{\text{had},\gamma}(s)}{4\pi\alpha^2/3s}$$

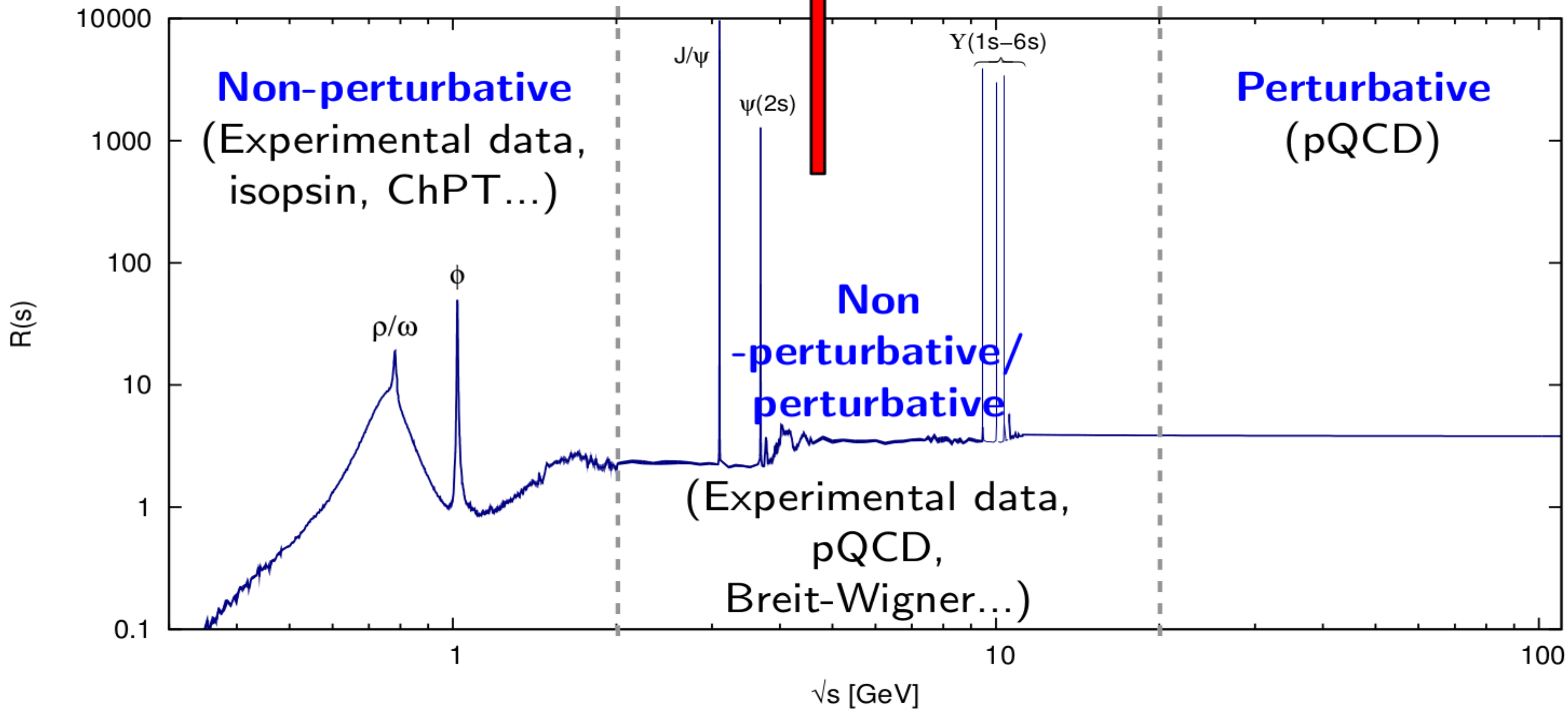

Must build full hadronic cross section/R-ratio...

Extra

3.6.1 Assignment of Bin-Errors

The contents of the bins is the sum total of the energy hits at that time in fill and the uncertainty comes from statistical uncertainty in the number of pulses that went into that bin, Δn_i, and also the statistical variation from the energy resolution in those pulses, E_i. The fluctuation in the energy value is considered to be a small contribution and is ignored in the uncertainty calculation. The total energy in a time bin of per calorimeter wiggle histograms given by

$$E_{total} = n_1 E_1 + n_2 E_2 + n_3 E_3 + ... \tag{3.2}$$

Ignoring the contribution from the fluctuation of energy per pulse, ΔE_i, the uncertainty for the corresponding bin would be

$$\Delta E_{total} = \sqrt{(E_1 \Delta n_1)^2 + (E_2 \Delta n_2)^2 + (E_3 \Delta n_3)^2} + ... \tag{3.3}$$

Assuming Poisson statistics and $\Delta n_i = \sqrt{n_i}$,

$$\Delta E_{total} = \sqrt{(E_1 \sqrt{n_1})^2 + (E_2 \sqrt{n_2})^2 + (E_3 \sqrt{n_3})^2} + ... \tag{3.4}$$

This is approximated as

$$\Delta E_{total} = \sqrt{(E_1)^2 + (E_2)^2 + (E_3)^2} + ... \tag{3.5}$$

where the effects from *pulse splitting*, that is sharing of a pulse energy between adjacent time bins, are ignored.